A COMPUTER IMPLEMENTATION OF THE STATIC AND DYNAMIC ANALYSIS OF INDUCED STRAIN ACTUATED BEAMS

by

Mahesh Kumar Subramaniam

Thesis submitted to the Faculty of the

Virginia Polytechnic Institute and State University

in partial fulfillment of the requirements for the degree of

MASTER OF SCIENCE

in

Mechanical Engineering

APPROVED:

Dr. Craig A. Rogers, Chairman

Dr. O. Hayden Griffin, Jr.

Dr. Larry D. Mitchell

Dr. Chen Liang

May, 1993

Blacksburg, Virginia

c.2

A Computer Implementation of the Static and Dynamic Analysis of Induced Strain Actuated Beams

by

Mahesh Kumar Subramaniam

Committee Chairman: Dr. Craig A. Rogers

Mechanical Engineering

Abstract

A generalized solution technique has been designed and developed for the static and dynamic analysis of induced strain actuated beam structures. A PC-based, user-friendly, menu-driven software program DAISA (Dynamic Analysis of Induced Strain Actuated Beams) has been developed for the analysis of structural response due to induced strain actuation, with a highly user-friendly interface. Transfer matrices have been used to generalize the beam problem to accommodate different boundary conditions, loading conditions due to an arbitrary number of symmetric actuator patches on the beam structure, structural damping effects, and the effects of stiffening and mass loading due to the presence of the actuators. DAISA has been designed to perform static-response, free-vibration, steady-state harmonic-response, and frequency-response analyses describing the structural response to induced strain actuation. Various modeling techniques, including the static, equivalent thermal expansion, and impedance approaches have been incorporated. DAISA has also been equipped to perform an electro-mechanical analysis of the beam-actuator system thereby providing adequate information about power consumption and

system power requirements. The algorithm and software presented in this thesis will serve to achieve better design considerations for actuators employed in structural and vibration control.

Acknowledgments

I would like to express my sincere appreciation and gratitude to my advisor, Dr. Craig Rogers for providing me encouragement and support throughout my graduate study. I would also like to thank Dr. Larry Mitchell for getting me interested in transfer matrices and his assistance at all times. I am extremely thankful to Dr. Chen Liang for providing me valuable support at the most difficult times. I would also like to thank Dr. Hayden Griffin for his time and advice.

A special thanks goes to all the students and staff at the Center for Intelligent Material Systems and Structures for making me feel at home during my stay at Virginia Tech. A special mention is due Dr. Zaffir Chaudhry for the many technical and personal discussions during my stay at CIMSS.

I would also like to acknowledge the support of the National Science Foundation Presidential Young Investigator Program, NSF Grant No. MSS-9157080, Dr. Ken Chong, Program Director; and the U.S. Army Research Office University Research Initiative Program, ARO Grant No. DAAL03-92-G-0180, Dr. Gary Anderson, Program Director.

I am greatly indebted to my parents for their constant prayers and support throughout my education. It is indeed true that this thesis would not have been a reality without them.

Table of Contents

List of Figures

List of Tables

Chapter 1

Introduction

Intelligent material systems have been identified as one of the most important emerging materials technology for numerous applications, both defense and commercial. They are expected to revolutionize presently available material systems by instilling intelligence in them. The intention of this chapter is to provide a clear definition of intelligent material systems, their applications, and the motivation for this research work.

1.1 Definition of Intelligent Material Systems

Intelligent material systems, sometimes referred to as smart materials or structures, are defined in the literature in the context of many different paradigms. According to Rogers (1992), one such definition is based on a technology paradigm: "the integration of actuators, sensors, and controls with a material or structural component". Another definition is based on a science paradigm: "material systems with intelligence and life features integrated in the micro structure of the material system to reduce mass and energy and produce adaptive functionality". The former definition describes the components that comprise a smart material system, but does not state the objective of the system nor the way to create such a material system. The latter definition states the objective of the material system, but does not define the type of materials to be used. However it is essential to note that the vision of intelligent material systems is universal: that of learning from nature and living systems and applying that knowledge in such a way as to enable

man-made objects to have the adaptive features of nature's creations.

1.2 Motivation

Active vibration and shape control of structures have become topics of interest in recent years with both industry and the engineering research community. Distributed induced strain actuators have been widely chosen to achieve control in structural vibration (Crawley and de Luis, 1987; Bailey and Hubbard, 1985; Fanson and Chen, 1986) and structural acoustics (Dimitriadis, Fuller and Rogers 1991). Induced strain actuation is the process by which actuation strain in some elements of a structure induces deformation of the overall structure. Incorporating such elements (in which actuation strain can be regulated) on a structure serves to effect vibration and structural control. A most commonly used induced strain actuation mechanism is piezoelectricity. Piezoelectricity is the phenomenon in which certain crystalline substances develop an electric field when subjected to pressure forces, or conversely, exhibit a mechanical deformation when subjected to an electric field. This reciprocal coupling between mechanical and electrical energy renders piezoelectric materials useful as both an actuator and sensor in many applications, especially in structural and vibration control. A potential application is their use as highly distributed actuators in intelligent structures (Crawley et al., 1988). With such distributed actuators, it is possible to design structures with intrinsic vibration and shape control capabilities.

To date, various analytical models have been developed to describe the mechanics of interaction between the actuator and the structure. Most of these models have been

developed on static considerations while some dynamic models have also been proposed. A clear understanding of the interaction between the actuator and the structure is essential in designing the actuators for typical applications. This calls for a solution technique for analyzing the static and dynamic interaction of the actuator-structure system. The focus of this research was to develop a generalized solution procedure for the static and dynamic analysis of induced strain actuated beam structures for the various available analytical models leading to better design considerations. This thesis can be perceived as a computer-aided design tool and an optimization tool for actuator-structure systems employed in structural and vibration control applications.

1.3 Applications

Most of the research has been concentrated in the area of vibration and acoustic control. A substantial reduction in vibration decay time was reported by using piezoelectric actuators as active dampers for beams (Bailey and Hubbard, 1985; Fanson et al., 1989). These investigations show that with such actuators a number of vibration modes can be simultaneously controlled with reduced spillover of energy into higher modes. Dimitriadis, Fuller, and Rogers (1991) investigated the behavior of a pair of two-dimensional piezoelectric patches surface-bonded to an elastic plate and used as distributed vibration actuators. It was shown that modes can be selectively excited and that the geometry of the actuator shape effects the modal distribution of the plate. Also the location of the piezoactuator was shown to effect significantly the vibration response of the plate. Shape memory alloy hybrid composites have also been successfully employed for vibration and acoustic control (Rogers, 1990; Anders, Rogers, and Fuller, 1991).

Piezoelectric actuators have also been used on composite and metal plates to effect shape control (Crawley and Lazarus, 1989). The possible use of piezoelectric actuators for actively changing the flap angle of a helicopter rotor blade has been studied (Spangler and Hall, 1990). The use of materials with large coefficient of thermal expansion has been suggested for controlling the deformation in large space structures (Haftka and Adelman, 1985). An optical control system with induced strain actuators has been constructed by mounting these actuators below the optical mirror surface to effect desired mirror curvatures and focal length (Chirappa and Claysmith, 1981).

The use of intelligent material systems for commercial applications can be visualized in the coming years although its use has been quite restricted to defense applications presently. It should be noted that this concept will revolutionize the process of building material systems. It will enable man-made inanimate objects to become more natural and liveable. According to Rogers (1992), intelligent material systems will be manifestations of the next materials and engineering revolution - the dawn of a new materials age.

Chapter 2

Analytical Models of Induced Strain Actuation

Induced strain actuators refer to materials that exhibit some sort of coupling between their geometric configuration and applied non-mechanical stimuli. Induced strain actuators derive their name from the fact that they cause localized strains on the structure on which they are mounted. Actuation strain is the general term for all sources of strain which enter the constitutive relations. Actuation strains may be due to a variety of effects as thermal expansion (Jones, 1975), piezoelectricity (Crawley and de Luis, 1987), electrostriction (Uchino, 1986), material phase change (Shimizu, et al., 1986), or magnetostriction (Butler, 1988). The actuation strain is the mechanism by which actuators induce strain and thereby effect control. Such actuators are assembled into systems either through surface bonding or embedding them in the structure themselves.

Currently, the most researched and used induced strain actuators are piezoceramics. These piezoceramic actuators are simple, compact, light weight structures which can be incorporated easily into induced strain actuator-structure systems. Piezoceramics produce actuation strains in response to applied electric fields.

Detailed models of induced strain actuator-structure systems have been developed. Commonly employed models are displacement-based models such as the pin-force model (Crawley, 1989), consistent plate model (Crawley, 1989), and the impedance model (Liang, Sun and Rogers, 1993).

2.1 Static Models

The static approach refers to the method of using a statically determined equivalent force or moment as the amplitude of the forcing function to determine the dynamic response due to the activation of integrated induced strain actuators. This force is determined using analytical models such as the Pin-force and the Bernoulli-Euler model as discussed in the following sections.

2.1.1 Pin-Force Model

The pin-force model conceptually models the induced strain actuators and the structure to be separate components, and can be used to evaluate the effectiveness of simple induced strain systems. Although this model does not correctly predict the actuator-structure response for thin structures (Chaudhry and Rogers, 1991), it provides an insight into the physics of induced strain actuation. The most basic induced strain actuator-structure systems are those composed of one-dimensional linear elastic bars actuated in extensional mode, and beams actuated in bending which are discussed in the following sections.

The pin-force model considers the actuator and the structure to be separate elastic bodies as shown in Figure 2.1. The extensional forces produced by the strain actuators are transferred to the substrate by pins at the edges of the actuators (Crawley and de Luis). This model of force transfer from actuator to substrate is consistent with the assumption of perfect bonding between the actuator and the structure.

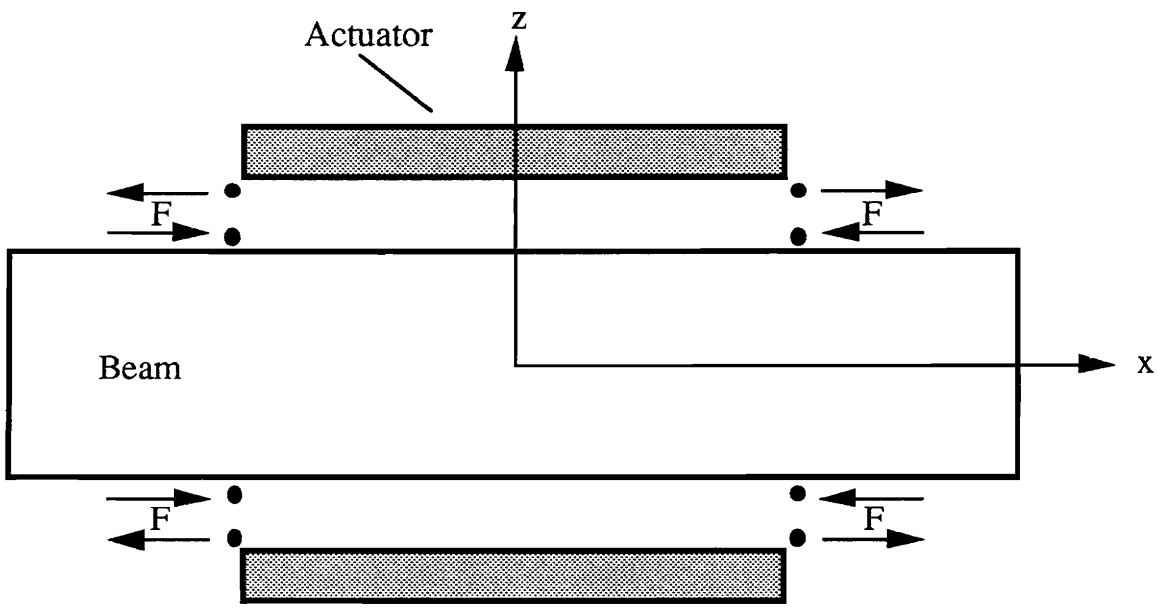

Figure 2.1: Pin-force model for a pair of symmetric actuators

Under the condition of perfect bonding, the shear stress σ_{xz} is concentrated in an infinitesimal zone at the end of the actuator, modeled by the pins. The pin connection allows for the strain in the actuator and the structure to be modeled independently, so long as strain compatibility is assumed at the location of the pins.

For a pure extension case, the strain in the structure is assumed to be uniform as shown in Figure 2.2. Assuming strain compatibility at the actuator-structure interface, the strain in the actuator is also assumed to remain constant through the thickness. The stress-strain relationships for the actuator and the structure are

$$\varepsilon_a = \frac{\sigma_a}{E_a} + \Lambda \tag{2.1}$$

$$\varepsilon_s = \frac{\sigma_s}{E_s} \tag{2.2}$$

The actuation strain Λ enters into the equations in the same manner as does the thermal strain, and the actuation strain is the strain which causes, physically, induced strains to be produced.

The equilibrium equations for the extensional case are

$$\sigma_a = -\frac{F}{bt_a} \tag{2.3}$$

$$\sigma_s = \frac{2F}{bt_s} \tag{2.4}$$

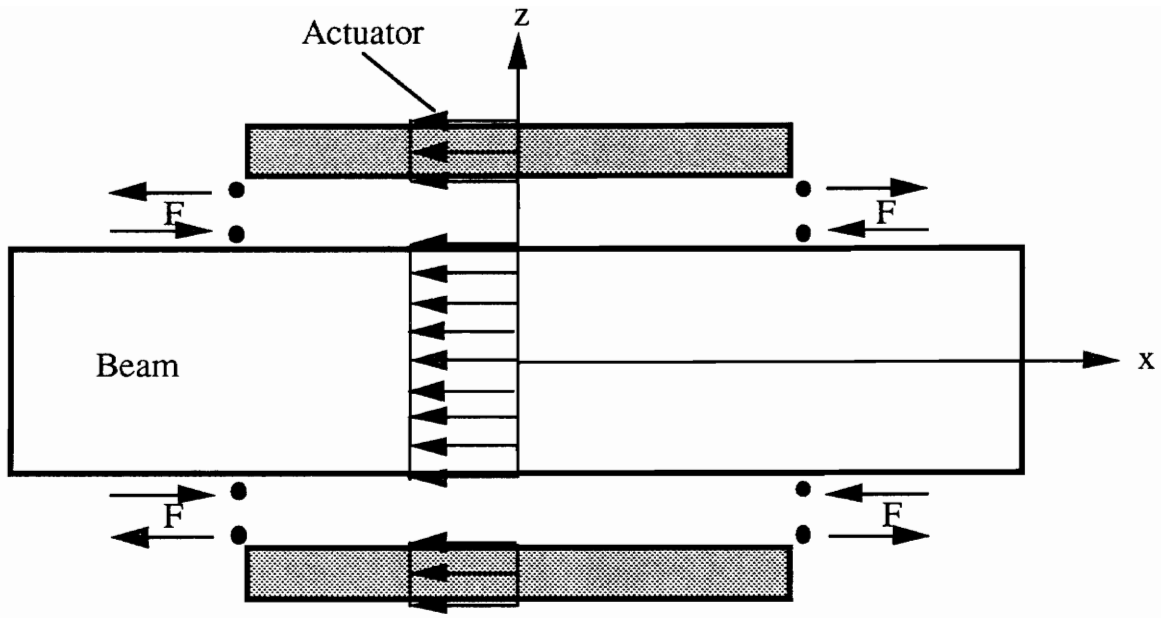

Figure 2.2: Pin-force model - Strain distribution for pure extension

In these equilibrium expressions σ is the stress which develops in the actuators or the structure and F is the force on the pins. By applying compatibility at the actuator-beam interface and substituting the equilibrium relationships into the stress-strain relations, the pin force can be calculated as

$$\frac{F}{b} = \left[\frac{1}{2+\psi}\right] E_s t_s \Lambda \tag{2.5}$$

The non-dimensional parameter ψ , referred to as the relative stiffness ratio, represents the stiffness of the structure compared to that of the actuator and is defined as

$$\psi = \frac{E_s t_s}{E_a t_a} \tag{2.6}$$

An expression for the resultant total strain in the actuator is found by substituting the pin-force expression back into the equilibrium equations and combining this result with the stress-strain relations as

$$\varepsilon_a = \left[\frac{2}{2+\psi}\right] \Lambda \tag{2.7}$$

It can be seen from the above relation that for any given actuator configuration, the induced strain in the structure can be increased by decreasing the stiffness of the structure relative to the actuator or by increasing the actuation strain.

For a pure bending case, the structure is assumed to deform only in bending thereby producing a pure moment. This is achieved by actuating the two induced strain actuators

out of phase with one another. One actuator produces an extensional actuation strain while the other produces a compressive actuation strain. The strain in the structure is assumed to vary linearly through the structure thickness and the strain in the actuator is constant through the actuator thickness as shown in Figure 2.3.

The moment curvature equation for the beam is

$$M = Ft_s = (EI)_s \kappa \tag{2.8}$$

The compatibility of strain at the interface is

$$-\frac{t_s}{2}\kappa = \varepsilon_a = \frac{F}{(AE)_a} + \Lambda \tag{2.9}$$

Substituting for the force F from Eq. (2.3) into Eq. (2.2), we can solve for the curvature induced in the beam as

$$\kappa = \frac{12\Lambda}{t_s(6+\psi)} \tag{2.10}$$

The total strain induced in the structure is given by

$$\varepsilon_s = \left[\frac{6}{6+\psi}\right]\Lambda \tag{2.11}$$

Thus, the expression for the strain induced in the structure can be generalized as

$$\varepsilon_s = \left[\frac{\alpha}{\alpha+\psi}\right]\Lambda \tag{2.12}$$

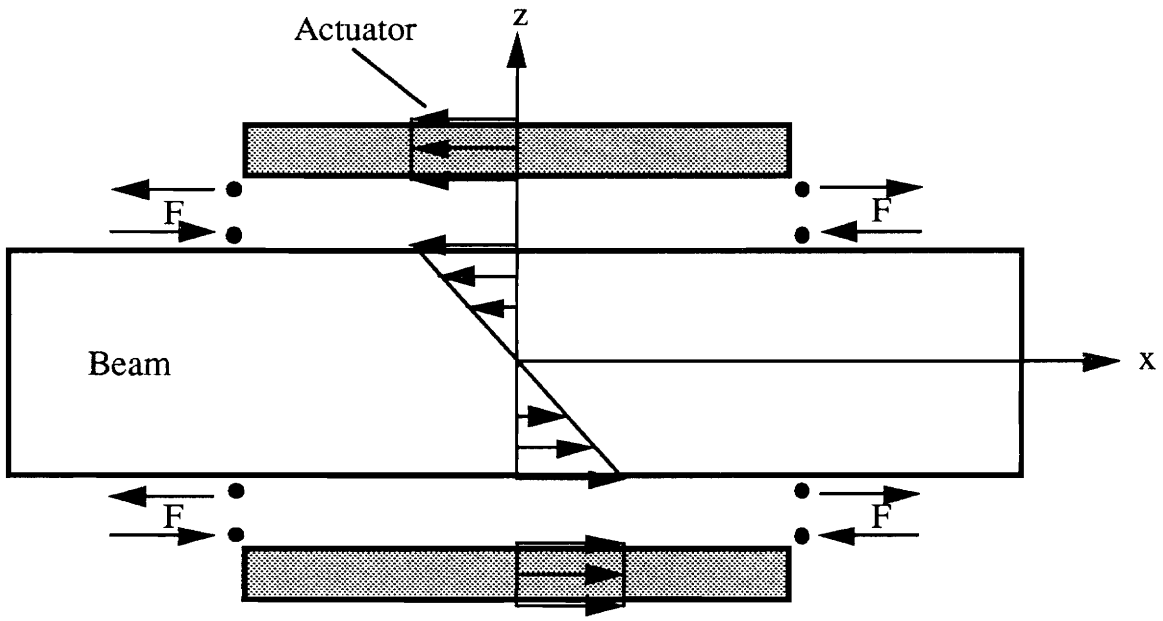

Figure 2.3: Pin-force model - Strain distribution for pure bending

where α is a constant which depends upon the geometry of the system and the mode of actuation. For bending actuation α is 6 and for extensional actuation α is 2.

It can be seen that Eq. (2.12) describing the transfer of actuation strain to induced strain is identical for both extensional and bending actuation, but the exact strain values for the two systems differ because of the geometry of the deformations. It can also be noted that the strain induced in the substrate is a function of the actuation strain Λ , relative stiffness ratio ψ , and the geometric constant α .

2.1.2 Bernoulli-Euler Model

This model considers both the actuators and the structure to be plies of a laminated plate as shown in Figure 2.4. The basic assumption used in thin plate theory is that the total plate thickness is much smaller than the longitudinal or transverse dimensions. This causes the stresses acting on the surface parallel to the mid-plane to be small compared to the in-plane stresses. Also, plane sections are assumed to remain plane and normal to the mid-plane during deformation.

Thin plate theory requires the out-of-plane deformations to be a function of only the longitudinal and transverse coordinates. Therefore the bending strains and curvatures, and the membrane strains can be fully described by derivatives with respect to these coordinates. The total strain of a thin plate is composed of a mid-plane strain ε^{o} and a curvature component κ .

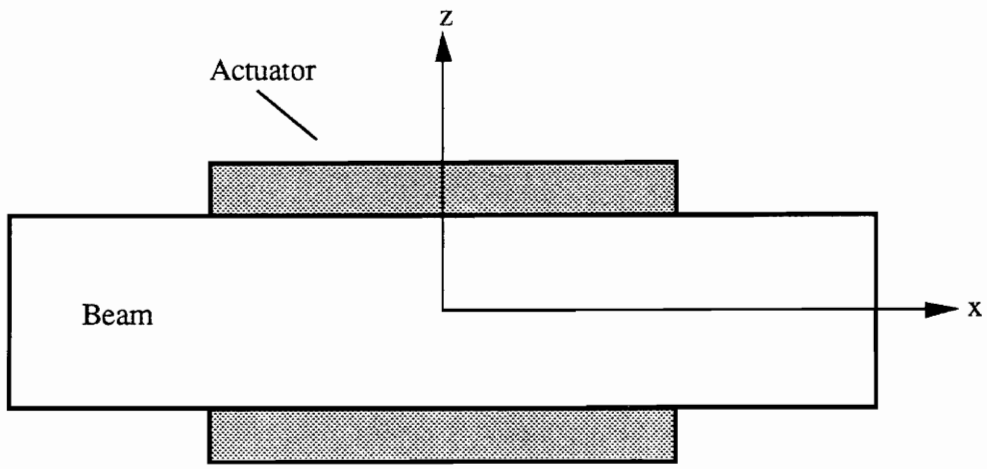

Figure 2.4: Bernoulli-Euler model for a pair of symmetric actuators

The strain is defined by the following strain-displacement relation

$$\varepsilon = \varepsilon^o + z\kappa$$

where z is the out-of-plane coordinate axis.

In the absence of externally applied loads, the resultant forces and moments due to the actuation strain are given by

$$P_\Lambda = (EA)_{total}\varepsilon^o - (ES)_{total}\kappa$$

$$M_\Lambda = (ES)_{total}\varepsilon^o - (EI)_{total}\kappa$$

where

$$(EA)_{total} = \int_z E(z)b(z)dz$$

$$(ES)_{total} = \int_z E(z)b(z)zdz$$

$$(EI)_{total} = \int_z E(z)b(z)z^2dz$$

are the total area stiffness, and the first and second moment of inertia, respectively.

For a pure extension case, a uniform strain distribution is assumed through the thickness of both the structure and the actuator as shown in Figure 2.5. Considering symmetric actuators for a pure extension case, the expression for the resultant force becomes

$$(EA)_{total}\varepsilon^o = P_\Lambda$$

Integrating over the thickness of the entire system, the mid-plane strain can be obtained as

$$\varepsilon^o = \left[\frac{2}{2+\psi}\right]\Lambda \tag{2.13}$$

In the case of pure bending, the strain is assumed to vary linearly through both the actuator and the structure as shown in Figure 2.6. Considering symmetric actuators for a pure bending case, the moment curvature relation becomes

$$-(EI)_{total}\kappa = M_\Lambda \tag{2.14}$$

Integrating over the thickness of the entire system, the mid-plane curvature is obtained as

$$\kappa = \frac{12\left(1+\frac{1}{T}\right)}{t_s\left(6+\psi+\frac{8}{T^2}+\frac{12}{T}\right)}\Lambda \tag{2.15}$$

where T is the ratio of the thickness of the structure to the actuator thickness.

This expression for curvature is different from that obtained by the pin-force model. Figure 2.7 shows the normalized curvature as a function of the beam-actuator thickness ratio t_s/t_a, for a modulus ratio E_s/E_a of one. It can be seen that for small thickness ratios, the pin-force model incorrectly predicts structure surface strains approaching actuation strains. It has been shown that such an incorrect prediction by the pin-force model is not due to the assumed uniform strain distribution in the actuator, but due to the incorrect moment curvature equation (Chaudhry and Rogers 1991). It can also be seen that the Bernoulli-Euler model correctly predicts the response of the actuator-structure system as the mass and stiffness effects of the actuator are considered in the computations.

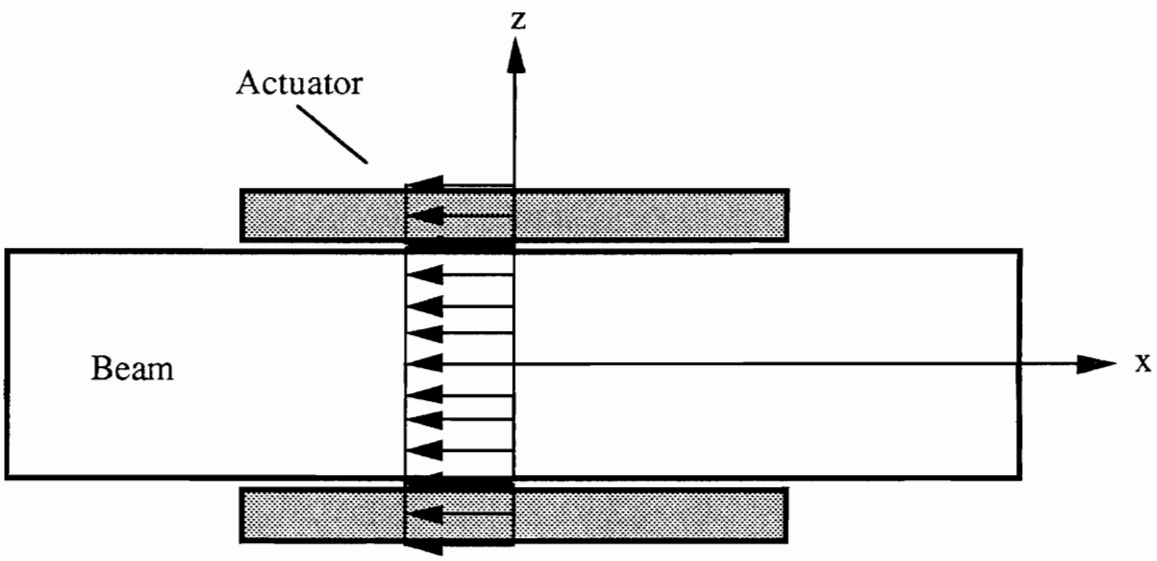

Figure 2.5: Bernoulli-Euler model - Strain distribution for pure extension

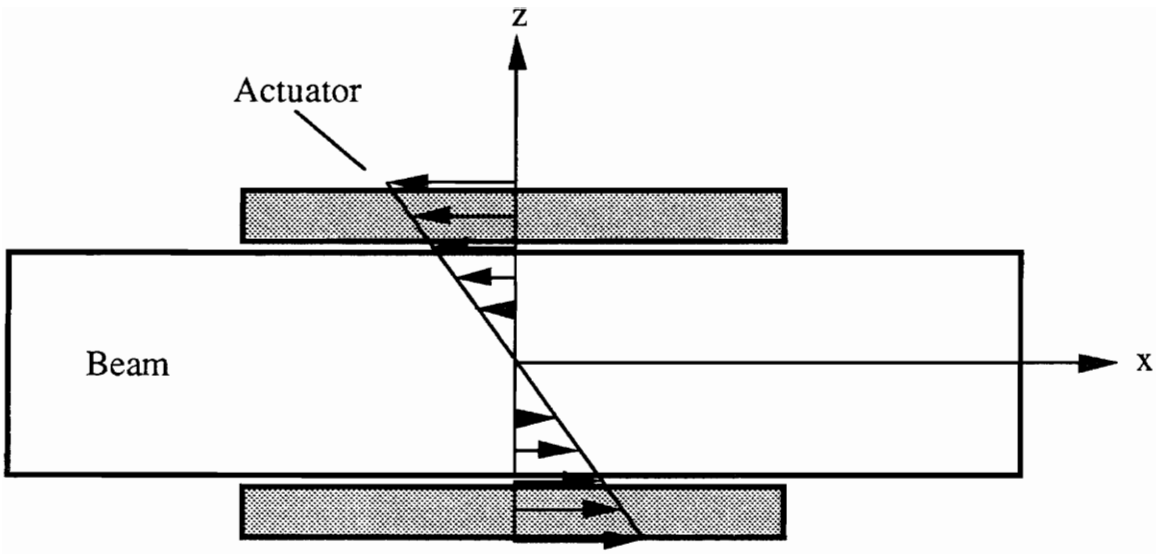

Figure 2.6: Bernoulli-Euler model - Strain distribution for pure bending

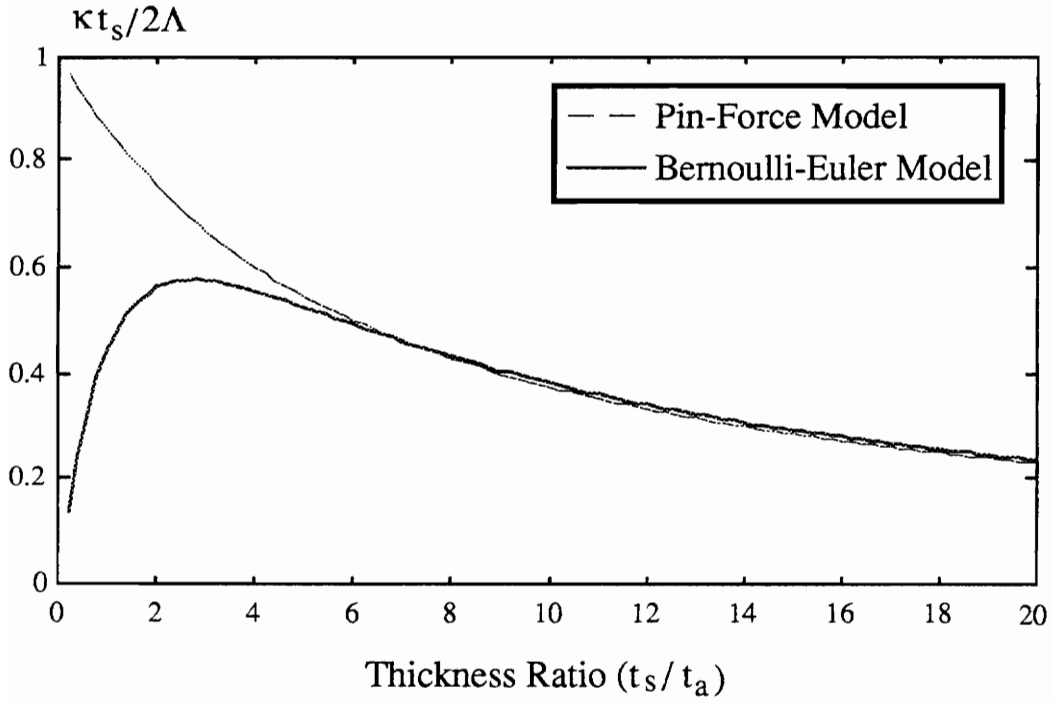

Figure 2.7: Normalized curvature vs. Thickness ratio

The electric induced strain from any induced strain actuator has the same effect as thermal expansion on the structure response. This fact gives rise to an equivalent thermal expansion model in which the equivalent force or moment (determined by the Pin-force and Bernoulli-Euler models) is replaced by an equivalent thermal force or moment as can be visualized in a thermal loading process. The resultant forces and moments due to the actuation strain are given by:

$$P_{\Lambda} = \int_{z} E(z)\Lambda(z)b(z)dz \tag{2.16}$$

$$M_{\Lambda} = \int_{z} E(z)\Lambda(z)b(z)zdz \tag{2.17}$$

Integrating Eqs. (2.16) and (2.17) yield the following expressions for the resultant forces and moments for the case of pure extension and pure bending respectively.

$$P_{\Lambda} = 2E_a b_a t_a \Lambda \tag{2.18}$$

$$M_{\Lambda} = E_a b_a t_a (t_a + t_s)\Lambda \tag{2.19}$$

This concept of equivalent thermal moment follows the assumptions underlying the Bernoulli-Euler approach, such as the actuators being treated as regular structure components with mass and stiffness. This model can be regarded as a variation of the Bernoulli-Euler model that can be exploited for both static and dynamic analysis for an accurate prediction of the structural response. It is important to note that this model provides an accurate description of the dynamic response of the actuator-structure system.

2.2 Impedance Model

The interaction between actuators and structures is governed by the dynamic output characteristics of actuators and the dynamic characteristics of structures, i.e., the structural impedance (Liang, Sun and Rogers, 1993). The interaction between an actuator and its host structure can be described using the structural mechanical impedance at the point where the actuator is integrated. This model provides a straightforward approach to accurately determine the dynamic response of active material systems. It represents the physical essence of the interaction between actuators and structures. As a discretized method, it can provide much more information compared with the other analytical models described in the previous sections.

2.2.1 Dynamic Analysis

The basic elements of this approach is illustrated by considering a PZT actuator-driven one-degree-of-freedom spring-mass-damper (SMD) system as shown in Figure 2.8 (Liang, Sun and Rogers, 1993). The electric field is applied in the z-direction and it is assumed that the PZT expands and contracts only in the y-direction. The constitutive relation of the PZT is expressed as below

$$S_2 = \overline{S}_{22}^{E} T_2 + d_{32} E \tag{2.20}$$

and

$$D_3 = \overline{\varepsilon}_{33}^{T} E + d_{32} T_2 \tag{2.21}$$

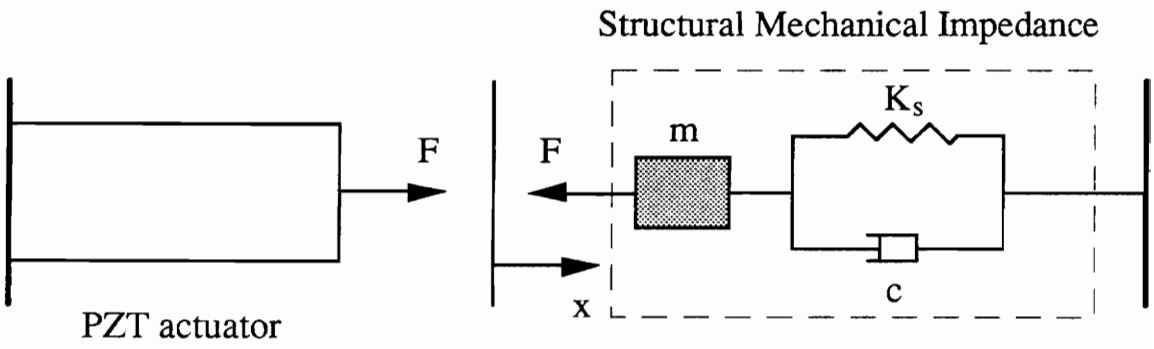

Figure 2.8: A PZT actuator driven one-degree-of-freedom spring-mass-damper system (Liang, Sun, and Rogers, 1993)

The equation of motion for a PZT vibrating in the y-direction is as below

$$\rho \frac{\partial^2 v}{\partial t^2} = \bar{Y}_{22}^E \frac{\partial^2 v}{\partial y^2} \tag{2.22}$$

Solving Eq. (2.22) by separating the displacement v into spatial and temporal domain solutions yield

$$v = \bar{v} e^{j\omega t} = (A \sin ky + B \cos ky) e^{j\omega t} \tag{2.23}$$

where

$$k^2 = \frac{\omega^2 \rho}{\bar{Y}_{22}^E}$$

If a constant force excitation is applied to the PZT actuator as shown in Figure 2.9 (Liang, Sun and Rogers, 1993), the actuator response can be determined from Eq. (2.23). The mechanical impedance of the PZT actuator is given by

$$z_A = -\frac{K_A(1 + j\eta)}{\omega} \frac{kl_A}{\tan(kl_A)} j \tag{2.24}$$

The mechanical impedance determined is based on the assumption that the PZT actuator behaves like a regular material and has no electric coupling. The electro-mechanical impedance of a PZT actuator can be determined based on external circuit conditions and the second constitutive relation of PZT. The PZT is connected to a structure which is represented by its impedance Z. The equilibrium and compatibility relation between the

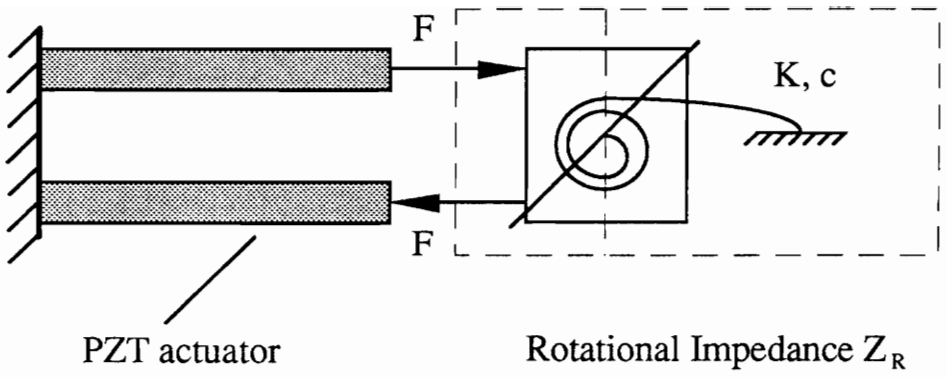

Figure 2.9: A simplified model for PZT actuators bonded on beam structures (Liang, Sun, and Rogers, 1993)

structure and the PZT is described by

$$T_{2\,y=l_A} = \overline{T}_{2\,y=l_A} e^{j\omega t} = -\frac{Z\overline{v}_{y=l_A} j\omega}{b_A t_A} e^{j\omega t} \tag{2.25}$$

This equation represents the structural impedance of a one-degree-of-freedom SMD system. Substituting Eq. (2.25) into Eq. (2.20) yields

$$\overline{S}_2 = \frac{d\overline{v}}{dy} = -\overline{S}_{22}^{E} \frac{Z\overline{v}_{y=l_A} j\omega}{b_A t_A} + d_{32} E \tag{2.26}$$

Equation (2.25) provides one boundary condition for Eq. (2.23). Another boundary condition $\overline{v}_{y=0} = 0$ leads to $B=0$. The coefficient A in Eq. (2.23) can be solved from Eq. (2.26) as

$$A = \frac{Z_A d_{32} \overline{E}}{k \cos(kl_A)(Z_A + Z)} \tag{2.27}$$

The output displacement of the PZT actuator and the stress, strain, electric displacement field are solved as below

$$\overline{x} = \overline{v}_{y=l_A} = \frac{Z_A d_{32} \overline{E} l_A}{Z_A + Z} \frac{\tan(kl)}{kl} \tag{2.28}$$

$$\overline{S}_2 = \frac{Z_A d_{32} \overline{E}}{Z_A + Z} \frac{\cos(ky)}{\cos(kl_A)} \tag{2.29}$$

$$\overline{T}_2 = \left(\frac{Z_A}{Z_A + Z} \frac{\cos(ky)}{\cos(kl_A)} - 1 \right) d_{32} \overline{Y}_{22}^{E} \overline{E} \tag{2.30}$$

$$\overline{D}_3 = \frac{Z_A \overline{Y}_{22}^E d_{32} \overline{E}}{Z_A + Z} \frac{\cos(ky)}{\cos(kl_A)} - \left(\overline{\varepsilon}_{22}^E - d_{32}^2 \overline{Y}_{22}^E\right)\overline{E} \tag{2.31}$$

The force output from the actuator is obtained as

$$\overline{F} = b_A t_A \overline{T}_{2_{y=l_A}} = -\frac{Z}{Z_A + Z} d_{32} \overline{E} \overline{Y}_{22}^E b_A t_A \tag{2.32}$$

The free stroke of the PZT actuator is obtained from Eq. (2.28) by assuming the mechanical impedance to be zero as

$$\overline{x}_f = d_{32} \overline{E} l_A \frac{\tan(kl_A)}{kl_A} \tag{2.33}$$

The dynamic blocking force is obtained from Eq. (2.32) by assuming an infinite mechanical impedance as

$$F_b = -\overline{Y}_{22}^E d_{32} \overline{E} b_A t_A \tag{2.34}$$

Equations (2.33) and (2.34) provide the dynamic output characteristics of PZT actuators. The force output from the actuator is its blocking force. The displacement output from the actuator is a function of frequency. If the PZT actuator is driving a mechanical system, the output force and displacement of the actuator are related as below

$$\overline{F} = K_A(1 + j\eta) \frac{\tan(kl_A)}{kl_A} \overline{x} + F_b \tag{2.35}$$

It can be seen that this force-displacement relation includes structural damping and the

dynamics of the actuator.

The actuator-structure interaction can now be explained using the concept of mechanical impedance match in Eq. (2.32). If the impedance of the mechanical system is at its lowest which corresponds to its resonance, the force provided by the actuator is at its lowest. If the structural impedance matches the actuator impedance, the actuator provides the maximum force. In order to use the impedance approach, the structural impedance corresponding to actuator loading must be calculated first. For actuators activated out-of-phase, resulting in a pure bending excitation, the rotational structural impedance is given by

$$Z_R = \frac{M_{eq}}{(\theta_i - \theta_{i-1})\, j\omega} \tag{2.36}$$

where θ_{i-1} and θ_i are the rotation angles at the ends of the actuators. The equivalent structural impedance given by Eq. (2.36) needs to be modified in order to be used in Eqs. (2.27) through (2.32). The interaction between the beam and the actuator can be represented by a simple system of two actuators creating a pure bending moment to drive a rotational spring-mass-damper system having the same rotational impedance as given by Eq. (2.36), as shown in Figure 2.5. The equivalent mechanical impedance that the actuators operate against is given by

$$Z = \frac{2Z_R}{t_s^2} \tag{2.37}$$

This impedance can be directly used in Eqs. (2.28) to (2.32) to determine the

displacement, strain, stress, electric displacement and force of the actuators respectively. Once the structural impedance corresponding to the actuator load is calculated, the stress within the actuators can be determined from Eq. (2.30). The actuator excitation can then be determined. This value of force or moment corresponds to the true excitation load. In the actual implementation of the impedance approach, the frequency-response-function is calculated first using a constant unit force or moment pair at the ends of the actuator depending on whether the actuators cause pure extension or pure bending. The actual dynamic response of the actuator-structure system can then be determined by multiplying this frequency-response-function with the true excitation load. In the case of multiple segmented actuators, the same procedure of applying a unit force or moment pair is performed over individual actuators and the dynamic response determined due to each actuator. The overall dynamic response of the actuator-structure system will be a superposition of the individual dynamic responses. The impedance approach provides an accurate description of the structural dynamic response due to the fact that the actual force/moment caused by the presence of the actuators is used in the computation. Thus the impedance model presents a general methodology for determining the dynamic response of active material systems.

2.2.2 Power Consumption

Integrated induced strain actuators provide energy for intelligent materials and structures to respond adaptively to internal and external stimuli. Energy transfer and consumption are very important issues in the application and design of intelligent material systems and structures. In a material system integrated with actuators, the power consumed by these

actuators consists of two parts: the power used to drive the system, which is dissipated as heat due to structural damping and the power dissipated by the actuators themselves due to the dielectric loss and internal damping, called the reactive power. A coupled electro-mechanical approach to analyze the energy transfer and consumption in adaptive structures has been presented (Liang, Sun, and Rogers, 1993).

Power consumption of actuators has become a very important issue in the design of active material systems. The fully coupled model developed serves to:

- determine the power supply required to operate the material system
- determine the energy efficiency of the material system
- determine the heat generated from the actuators to assist in the thermal stress analysis of induced strain actuators
- aid in the design of energy-efficient active material systems
- aid in the understanding of system energy transfer.

The electro-mechanical modeling of PZT actuator driven systems follows the impedance approach discussed in the previous section. A simple piezoelectric ceramic driven one-degree-of-freedom spring-mass-damper system as presented in section 2.2.1 is investigated. If a voltage, $V = V \sin(\omega t)$ is applied to a load, the current measured in the circuit is $I = I \sin(\omega t + \phi)$. The voltage and current are related by the complex admittance

$$Y = \mathrm{Re}(Y) + j\,\mathrm{Im}(Y) \tag{2.38}$$

The three types of power are discussed as follows:

The apparent power is the power supplied and is expressed as:

$$W_A = I_e V_e = \frac{V^2}{2}|Y| \tag{2.39}$$

where I_e and V_e are the RMS current and voltage respectively.

The dissipative power is the power transformed into other energy forms and is expressed as:

$$W_D = W_A \cos\phi = \frac{V^2}{2}\mathrm{Re}(Y) \tag{2.40}$$

The reactive power remains and flows in the system. It consists of a mechanical reactive power related to mass (kinetic energy), spring (potential energy), and electric reactive power (electric and magnetic field energy of capacitors and inductors). It is expressed as:

$$W_R = W_A \sin\phi = \frac{V^2}{2}\mathrm{Im}(Y) \tag{2.41}$$

The power consumption of a PZT actuator powered by a constant voltage source varies because of the variation of Re(Y) as a function of frequency. In order to maintain a constant voltage supply for the PZT actuator at various frequencies, the maximum power rating of the voltage source should be no less than

$$W_{rating} = \frac{V^2}{2}\max(|Y|) \tag{2.42}$$

The real admittance has two parts. One part is due to the damping of the mechanical system which is useful in terms of driving the mechanical system. The other part is due to

the dielectric loss and mechanical loss of the PZT which is dissipated in terms of heat generated in the PZT. The efficiency of the actuator in driving the system is defined as:

$$\phi = \frac{\mathrm{Re}(Y_s)}{\mathrm{Re}(Y)} \tag{2.43}$$

where Y_S is the admittance obtained by assuming zero dielectric loss and internal damping for the PZT actuators. Similarly Y_a is the admittance with zero structural damping. By energy conservation

$$\mathrm{Re}(Y) = \mathrm{Re}(Y_s) + \mathrm{Re}(Y_a) \tag{2.44}$$

The electric current is expressed by the following relation

$$I = j\omega \iint D_3 dxdy \tag{2.45}$$

which yields

$$I = \bar{I} e^{j\omega t} \tag{2.46}$$

where

$$\bar{I} = j\omega \bar{E} b_a l_a \left(\frac{d_{32}^2 \bar{Y}_{22}^E Z_A}{Z + Z_A} \frac{\tan(kl_a)}{kl_a} + \bar{\varepsilon}_{33}^T - d_{32}^2 \bar{Y}_{22}^E \right) \tag{2.47}$$

The coupled electro-mechanical admittance is defined as:

$$Y = j\omega \frac{b_a l_a}{t_a} \left(\frac{d_{32}^2 \bar{Y}_{22}^E Z_A}{Z + Z_A} \frac{\tan(kl_a)}{kl_a} + \bar{\varepsilon}_{33}^T - d_{32}^2 \bar{Y}_{22}^E \right) \tag{2.48}$$

The quantity $\tan(kl_a)/kl_a$ is unity in the frequency range of interest in most applications of active material systems. Then Eq. (2.48) becomes

$$Y = j\omega \frac{b_a l_a}{t_a}\left(\bar{\varepsilon}_{33}^{T} - \frac{Z}{Z+Z_A} d_{32}^2 \bar{Y}_{22}^{E}\right) \tag{2.49}$$

It is clear that the coupled electro-mechanical admittance includes the capacitance of the PZT material and the mechanical interaction expressed by the mechanical impedance terms. The resonance of the electro-mechanical system occurs when the actuator and structural impedance match.

It can be seen that the impedance model clearly describes the physics underlying the actuator-structure interaction. It should also be noted that this model, besides describing the dynamic interaction between the actuator and the structure also serves to perform an electro-mechanical analysis to determine electrical parameters such as actuator power consumption and system power requirement. Thus, the impedance model can be regarded as a possible means of studying the energy consumption and transfer in an active material system, which has been a long-standing issue in the smart material system community.

Chapter 3

Transfer Matrix Method

The Transfer Matrix Method (TMM) is based on the idea that a continuous and/or complicated system can be broken up into component parts with simple elastic and dynamic properties that can be expressed in matrix form. These component matrices are considered as building blocks that, when fitted together according to a set of predetermined set of rules, provide the static and dynamic properties of the entire system.

For a given beam with several sections, say i, each element or section is represented by the appropriate field and point matrices. The state vectors from the left end, $\{z\}_0$, to the right end, $\{z\}_i$, are related by the equation,

$$\{z\}_i = \{P\}_i[F]_i\{P\}_{i-1}[F]_{i-1}.....\{P\}_j[F]_j.....\{P\}_1[F]_1\{z\}_o = [U]\{z\}_o$$

where $[F]_j$ = a field transfer matrix that describes the j^{th} section of finite length.

$[P]_j$ = a point transfer matrix that describes the j^{th} element at a point

The state vector, $\{z\}$, has four components defined as:

$$\{z\} = \begin{Bmatrix} w \\ \theta \\ M \\ V \end{Bmatrix}$$

where w = transverse deflection, m

θ = slope, radian

M = moment, N-m

V = shear, N

The boundary conditions are as follows:

For pinned end, $w = 0$, $M = 0$

For fixed end, $w = 0$, $\theta = 0$

For free end, $M = 0$, $V = 0$

With a knowledge of the field and point matrices and the boundary conditions at the ends of the beam, the system characteristic equation can be assembled by in-line matrix multiplication of field and point matrices and the initial state vector $\{z\}_0$ can be computed. Once this is known, the matrix multiplication process is repeated to yield the state at each desired point along the beam. In fact, evaluation of the field matrices within their spatial realm allows for many more station state vector evaluators. This gives a better resolution of the states within the beam.

3.1 Static-Response Analysis

The deflection problem of a beam is often times complicated due to the geometry, loading conditions, and the presence of multiple supports. It is difficult to solve such beam problems using classical methods. Graphical integration was employed in the past to solve such problems. However, with the emergence of the transfer matrix method, this problem

has been simplified to a great extent. The main advantage of the method lies in the accuracy of its solutions for static deflection of beams and its ability to be extended to dynamic or vibration problem solutions. Moreover, the method allows the use of continuum structure models. These yield more accurate results than the discretized finite element method (FEM) procedures used in commercial modeling codes.

At this juncture, it is essential to understand several terms. The *state* of the beam is defined as the deflections of and the internal loads in the beam at the point of interest. The description of the state is done by a *state vector*. In matrix description,

$$\{z\}_{i-1} = \begin{Bmatrix} w \\ \theta \\ M \\ V \end{Bmatrix}_{i-1}$$

The state vector to the right of point *i-1* must be related to the state vector to the left of point *i* as shown in Figure 3.1 (Mitchell, 1991). By summing the vertical forces and moments about the point *i-1*, the relations for shear and moment are obtained respectively.

$$\sum F_y = 0 = V_i^L - V_{i-1}^R = 0$$
$$V_i^L = V_{i-1}^R \tag{3.1}$$

$$\sum M_{i-1} = 0 = M_i^L - M_{i-1}^R - V_i^L l_i$$
$$M_i^L = M_{i-1}^R + V_i^L l_i = M_{i-1}^R + V_{i-1}^R l_i \tag{3.2}$$

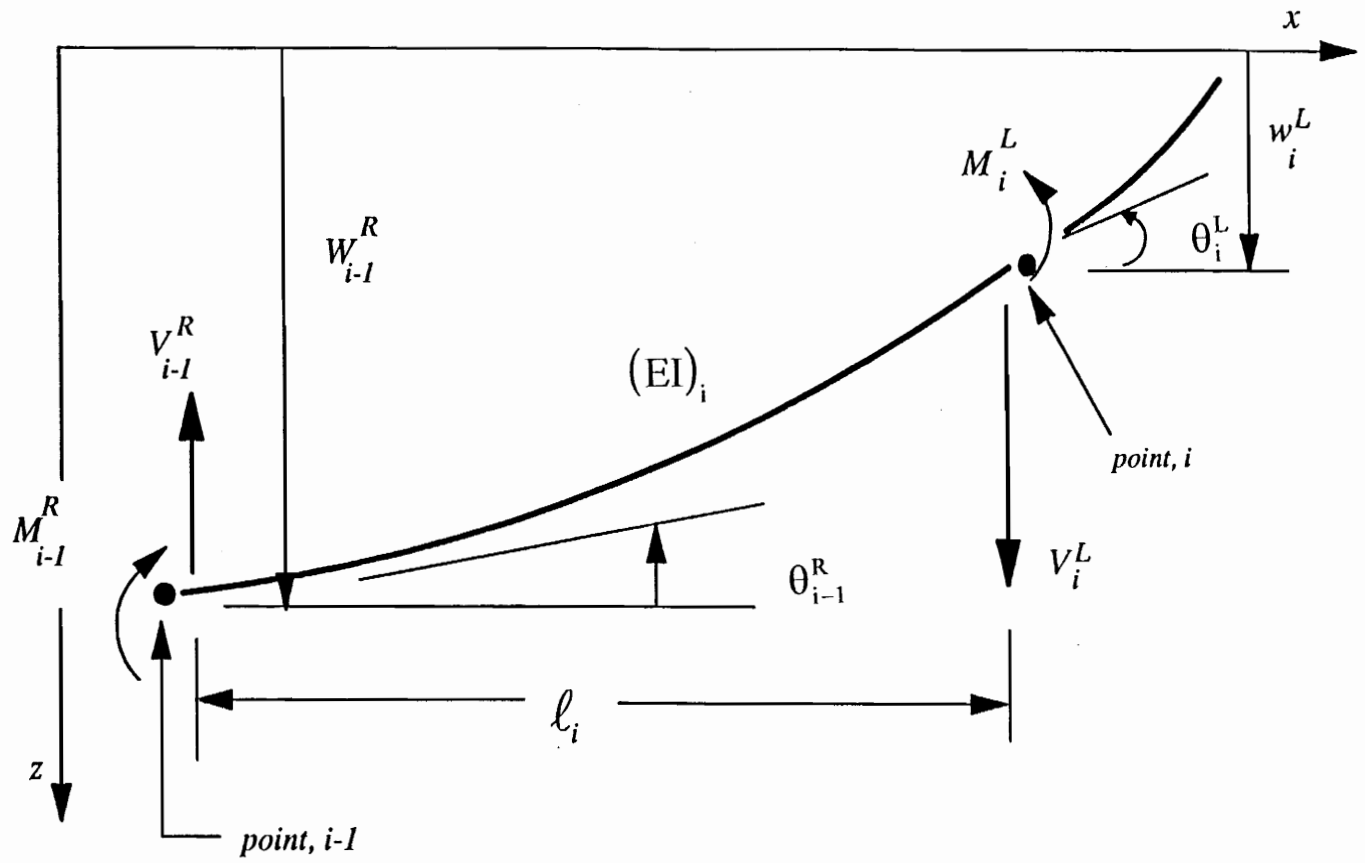

Figure 3.1: End forces and deflections for a massless elastic beam

The deflection relations are obtained by the method of superposition as depicted in Figure 3.2 (Mitchell, 1991).

$$w_i^L = w_{i-1}^R - \theta_{i-1}^R l_i - \frac{V_i^L l_i^3}{3EI} - \frac{M_i^L l_i^2}{2EI} \tag{3.3}$$

Substituting Eqs. (3.1) and (3.2) into Eq. (3.3), yields

$$w_i^L = w_{i-1}^R - \theta_{i-1}^R l_i - \frac{M_{i-1}^R l_i^2}{2EI} - \frac{V_{i-1}^R l_i^3}{6EI} \tag{3.4}$$

Differentiating Eq. (3.4) with respect to x gives the slope as

$$\theta_i^L = \theta_{i-1}^R + \frac{M_{i-1}^R l_i}{EI} + \frac{V_{i-1}^R l_i^2}{2EI} \tag{3.5}$$

Assembling Eqs. (3.1), (3.2), (3.4), (3.5) into a matrix form provides the transfer matrix for a massless elastic beam. This is known as the field transfer matrix, $[F_{beam}]$. The transfer matrix for the beam is a 4 by 4 matrix due to the inherent fourth order of the governing equation.

$$\begin{Bmatrix} w \\ \theta \\ M \\ V \\ 1 \end{Bmatrix}_i^L = \begin{bmatrix} 1 & -l_i & \frac{-l_i^2}{2EI} & \frac{-l_i^3}{6EI} & 0 \\ 0 & 1 & \frac{l_i}{EI} & \frac{l_i^2}{2EI} & 0 \\ 0 & 0 & 1 & l & 0 \\ 0 & 0 & 0 & 1 & 0 \\ 0 & 0 & 0 & 0 & 1 \end{bmatrix} \begin{Bmatrix} w \\ \theta \\ M \\ V \\ 1 \end{Bmatrix}_{i-1}^R \tag{3.6}$$

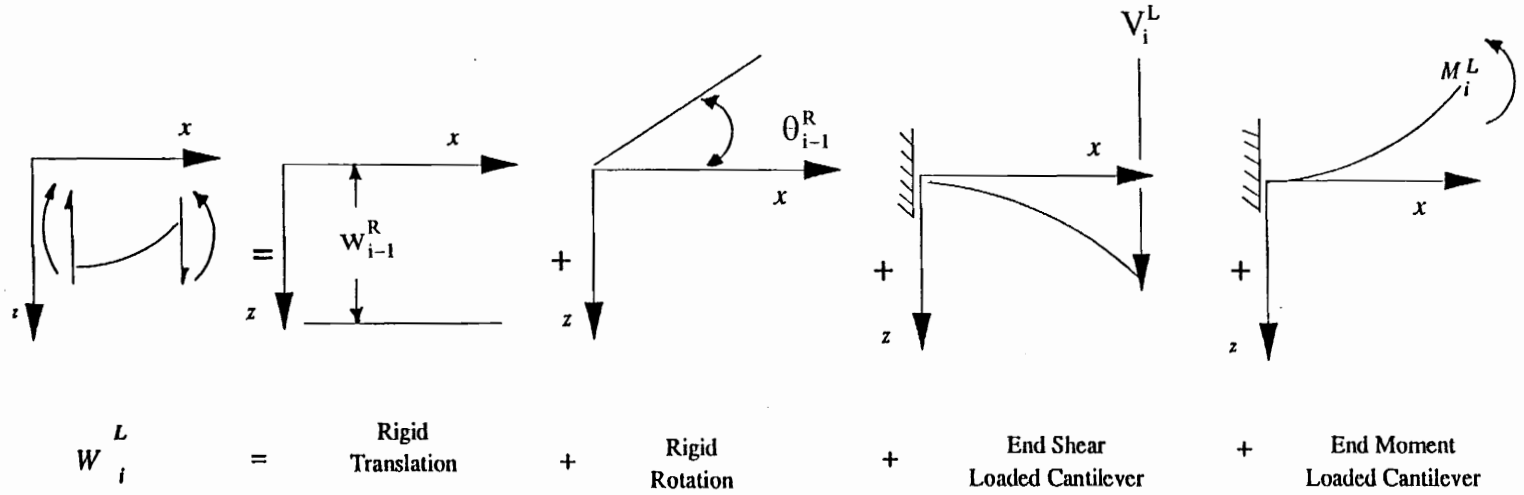

Figure 3.2: A superposition solution of the beam problem

With a knowledge of the overall transfer matrix and the boundary conditions of the beam, the initial parameters are determined. The state vector at any point on the beam can be determined by replacing l in the field matrix by $(x\text{-}a_i)$, where x and a_i are the distances of the point of interest from the left end of the beam and the start of the i^{th} element, respectively. The field transfer matrix of an element is given by:

$$L(x,a_i)=\begin{bmatrix} 1 & -(x-a_i) & \dfrac{-(x-a_i)^2}{2EI} & \dfrac{-(x-a_i)^3}{6EI} & 0 \\ 0 & 1 & \dfrac{(x-a_i)}{EI} & \dfrac{(x-a_i)^2}{2EI} & 0 \\ 0 & 0 & 1 & (x-a_i) & 0 \\ 0 & 0 & 0 & 1 & 0 \\ 0 & 0 & 0 & 0 & 1 \end{bmatrix} \tag{3.7}$$

External loading conditions, cross-sectional area changes, in span occurrences can be taken care of by introducing an *extended point matrix* $P(a_i)$ which is of zero length. The point matrix for a concentrated moment is given below:

$$P(x)=\begin{bmatrix} 1 & 0 & 0 & 0 & 0 \\ 0 & 1 & 0 & 0 & 0 \\ 0 & 0 & 1 & 0 & M \\ 0 & 0 & 0 & 1 & 0 \\ 0 & 0 & 0 & 0 & 1 \end{bmatrix} \tag{3.8}$$

where M is the value of the concentrated moment at point x.

3.2 Free-Vibration Analysis

It is quite important to determine the natural frequencies of the system being dealt with, in this case the system being the beam. The problem being an eigen-value problem involves the determination of the roots of the characteristic equation of the system. These roots correspond to the natural frequencies of the system. Forcing terms such as external loads on the beam are not taken into account since the natural frequencies and mode shapes are sought and not the steady-state response.

The overall transfer matrix and the initial parameters are determined. Application of the boundary conditions will provide two equations in four unknowns. However, two unknowns are eliminated due to the presence of homogeneous boundary conditions. This gives two equations in two unknowns. For a non-trivial solution the determinant of the matrix of these two equations should be zero. This provides the characteristic equation. Solving this characteristic equation iteratively yields the roots of the equation, namely the natural frequencies of the system. The mode shapes are obtained by assuming a unit value for one of the remaining two unknowns at the start of the beam. It should be noted that the choice of the unknown is arbitrary. The fourth unknown variable can then be determined. These values can then be used to determine the mode shape of the beam.

3.3 Steady-State Harmonic-Response Analysis

The evaluation of the dynamic-response of a structure requires the addition of a mass or inertial term to the equations of motion as well as a phased forcing function. In the static

response case the applied loads could be either up or down on the beam. However, with a dynamic excitation the harmonic forcing phasors can have various lead or lag phase angles with respect to one another (in the presence of damping). Thus the solution of the dynamic-response problem is identical to that of the static-response except that the series of transfer matrices must have inertia integrated into the point and/or field matrices at some point within the beam.

A steady-state solution is sought assuming harmonic excitation of the beam at a certain frequency. The field transfer matrix will now contain continuous mass terms as below

$$DL(x,a0)=\begin{bmatrix} e_1 & -e_2 & \frac{-e_3}{EI} & \frac{-e_4}{EI} & 0 \\ -\beta^4 e_4 & e_1 & \frac{e_2}{EI} & \frac{e_3}{EI} & 0 \\ -\rho\omega_i^2 e_3 & \rho\omega_i^2 e_4 & e_1 & e_2 & 0 \\ -\rho\omega_i^2 e_2 & \rho\omega_i^2 e_3 & \beta^4 e_4 & e_1 & 0 \\ 0 & 0 & 0 & 0 & 1 \end{bmatrix} \tag{3.9}$$

where

$$\beta_j^4=\frac{\omega_j^2\rho}{EI}$$

$$e_1=\frac{1}{2}\left[\cosh(\beta_j(x-a_i))+\cos(\beta_j(x-a_i))\right]$$

$$e_2=\frac{1}{2\beta_i}\left[\sinh(\beta_j(x-a_i))+\sin(\beta_j(x-a_i))\right]$$

$$e_3 = \frac{1}{2\beta_i^2}\left[\cosh(\beta_j(x-a_i)) - \cos(\beta_j(x-a_i))\right]$$

$$e_4 = \frac{1}{2\beta_i^3}\left[\sinh(\beta_j(x-a_i)) - \sin(\beta_j(x-a_i))\right] \tag{3.10}$$

External loads become harmonically varying loads and enter the point matrix. Use of this dynamic field transfer matrix along with point matrices to account for external loading conditions allows the determination of the overall dynamic transfer matrix. Initial parameters are calculated and the dynamic-response of the beam is obtained by in-line matrix multiplications of the dynamic field transfer matrices and point matrices along the length of the beam.

3.4 Frequency-Response Analysis

The solution procedure for this analysis is similar to the steady-state harmonic-response analysis except that the state vector at a given location of the beam is sought over a specified frequency range. The beam states are then plotted versus frequency.

3.5 Structural Damping

Real systems do not possess perfectly elastic springs, nor are they surrounded by a frictionless medium, and indeed they are often equipped with energy-dissipating elements. Structural damping is commonly employed in the investigation of steady state response of structures. It is introduced into the elastic solution by replacing the Young's modulus by

its complex form $E(1+j\gamma)$ where γ is the structural damping coefficient. The state vectors and transfer matrices can be separated into its real and imaginary parts as

$$S = S^r + jS^i$$
$$L = L^r + jL^i \tag{3.11}$$

where the superscripts r and i indicate real and imaginary parts. Such forms of state vectors and transfer matrices can be handled in precisely the same fashion as their usual counterparts.

Damped dynamic-response analysis and frequency-response analyses follow the same procedures listed in the previous sections, the only difference being that all computations are done in complex form. These provide complex results carrying the magnitude and phase or the real and the imaginary parts of the solution.

Transfer matrices offer a powerful solution procedure for the static and dynamic analysis of beam structures. Intermediate conditions, boundary conditions and number of degrees of freedom present no difficulty as they have no effect on the order of the transfer matrices required. In fact, their size is dependent only on the order of the differential equations governing the behavior of the elements of the system. Furthermore they lend themselves well to digital computers. It should however be noted that more elements in the model leads to more matrix multiplication and the accumulated numerical error in the multiplications can cause processor problems at higher frequencies and higher modes.

Chapter 4

Computer Implementation

A dedicated software DAISA has been developed for the static and dynamic analysis of induced strain actuated beam structures. The aim of this chapter is to provide a clear understanding of the various methods of analyses and their implementation schemes. A few illustrative examples are provided with the intention of getting the user started.

4.1 Problem Definition

The increasing use of actuators as elements of intelligent material systems require a thorough understanding of the dynamic interaction between the actuators and the structures on which they are mounted. Analytical models developed to date assume the mass of the actuator as negligible compared to the total mass of the system. Also, since any resonances of the actuator are much higher than the frequencies of interest, the actuator is assumed to act quasi-statically compared to the structure. It follows that the mechanical dynamics of the actuator can be ignored and the static models can be used to examine the influence of the actuator on the dynamics of the structure. A coupled dynamic model is required to describe the dynamic interaction between the actuator and the structure. A generalized computer implementation scheme is sought to describe the dynamic interaction of the actuator-structure system with the following assumptions:

- Beam is homogenous and isotropic
- Symmetric actuators are surface mounted
- Perfect bonding exists between the actuator and the beam

- Actuators are excited in pure extension or pure bending.

The following analytical models have been incorporated:

- Pin Force model or Static model
- Equivalent thermal expansion model
- Impedance model.

The computer software developed is capable of performing the following analyses:

- Static-response analysis
- Free-vibration analysis
- Damped / undamped steady-state harmonic-response analysis
- Damped / undamped frequency-response analysis.

4.2 Implementation Schemes

With the assumptions listed in the previous section and the theory of transfer matrices described in Chapter 3, an attempt is made to provide an insight into the schemes and procedures of implementation for the various analyses in the following sections.

4.2.1 Static-Response Analysis

This analysis seeks to obtain the state vector, namely the vector of displacement, slope, moment, and shear over the length of the beam. A massless beam is considered for the analysis. The presence of the actuators are modeled as extensional, compressive force

pairs or moment pairs concentrated at the ends of the actuators depending on whether they cause pure extension or pure bending. The loading effect due to the forces or moments is taken care of by the inclusion of respective point matrices (matrices of zero length). In-line matrix multiplication of field and point matrices yield the state vector at every point along the length of the beam.

4.2.2 Free-Vibration Analysis

This analysis seeks to obtain the natural frequencies of the actuator-beam system. External loading due to the actuators is not considered. The problem is no more than an eigen-value problem. The eigen-values of the system correspond to the natural frequencies of the system and the eigen-vectors correspond to the mode shapes. Since the frequency determinant varies logarithmically with frequency for the class of beam problems being analyzed, the frequency is incremented logarithmically so as to capture the exact frequency determinant curve with fewer iterations than if linear stepping is used. Extraction of the roots of the characteristic equation is done using the method of false position. For a damped system, the roots become complex conjugates. In such a case, Müller's method can be adopted for the extraction of the complex eigen-values.

4.2.3 Steady-State Harmonic-Response Analysis

This analysis is designed to determine the state vectors along the length of the beam at a particular value of excitation frequency. A continuum beam is considered as in a free vibration analysis. The loading is assumed to vary harmonically in time. For example, for a

pure bending case (moment = M), the loading becomes M Sin ωt. This harmonic variation enters the solution procedure through the dynamic field transfer matrix. This analysis serves to determine the state of the beam at any excitation frequency.

4.2.4 Frequency-Response Analysis

This analysis is similar to the steady-state harmonic-response analysis except that the state vectors are determined at a particular position on the beam over a specified frequency range. A continuum beam is used in this case too.

4.3 DAISA

The software DAISA (Dynamic Analysis of Induced Strain Actuated Beams) has been developed in the DOS™ environment using Turbo Pascal™ and TEGL Windows Toolkit for Pascal. Table 4.1 presents the various mouse and keyboard operations associated with the use of DAISA. These operations are quite similar to those available in Windows™ applications, which aids in easy understanding and use of DAISA. This section serves as a user's guide in describing the various features of DAISA with illustrative figures.

Some of the analytical models are constrained to perform certain analyses only, due to the methodology used in their formulations. Tables 4.2 and 4.3 list the possible analyses that can be performed for each model and the corresponding plots for the various analyses. Check marks are used in these tables to indicate realistic combinations.

Table 4.1: Discussion of mouse and keyboard operations

Operation	Mouse	Keyboard
Choose a menu item	Click the left mouse button on the menu item (highlighted).	Press ALT + underlined letter of the desired menu item. Note: No two menu items have the same underlined letter.
Close a menu item	Click the right mouse button on the menu item.	Press ESC.
Choose a command under a menu item	Click the left mouse button on the command (highlighted).	Press the underlined letter of the desired menu item. Note: Commands under different menu items may have the same underlined letter.
Close a window	Double click on the left top corner of the window.	Press ALT + spacebar to open the control menu box. Then press C.
Move a window	Hold the left mouse button on the window title bar, drag it to the new location and release the mouse button.	

Table 4.2: Model - Analysis Relationship

Analysis / Model	Static-Response	Free-vibration	Dynamic-Response	Frequency-Response
Static	X	X	X	X
Equivalent Thermal Expansion	X	X	X	X
Impedance	-	-	X	X

Table 4.3: Analysis - Plots Relationship

Model / Plots	Static	Equivalent Thermal Expansion	Impedance
Static Moment	X	X	-
Static Deflection	X	X	-
Dynamic-Response	X	X	X
Frequency-Response	X	X	X
Impedance	-	-	X
Admittance	-	-	X
Power Factor	-	-	X

Consider a cantilever beam with input parameters as listed in Table 4.4. Symmetric actuator patches are surface mounted near the fixed end of the beam and activated out of phase at 100 volts.

Entering **DAISA** at the DOS prompt will get the user to a dialog window as shown in Figure 4.1, which provides the option to *Continue* or *Quit* the program. Accepting to continue leads to the main program window with pull-down menus. Figures 4.2 through 4.5 explain the specification of input parameters for the problem. It has to be noted that two or more screen plots have been superposed to provide these figures to enable a better understanding of the sequence of operations. A logical sequence of operations for any analysis is presented below:

- Set physical and material properties of the beam structure
- Set physical and material properties of the actuator material
- Set boundary conditions
- Set actuator location and activation level
- Define analytical model
- Define analysis type
- Post process results.

Figure 4.6 shows the selection of the static model. With this model, a static-response analysis is performed as shown in Figure 4.7 and associated graphical plots provided in Figures 4.8 and 4.9.

Table 4.4: Input parameters for tutorial problem

Beam Data	Actuator Data
Young's Modulus, E_s = 6.895 x 10^{10} N/m^2	Young's Modulus, E_a = 6.274 x 10^{10} N/m^2
Density, ρ_s = 2693.42 kg/m^3	Density, ρ_a = 7633.945 kg/m^3
Structural damping coeff., γ_s = 0.001	Mechanical loss factor, γ_a = 0.000
Length, l_s = 0.3048 m	Piezoelectric coeff. d_{31} = -170 x 10^{-12} m/V
Width, b_s = 0.0254 m	Piezoelectric coeff. d_{32} = -170 x 10^{-12} m/V
Thickness, t_s = 0.0016637 m	Length, l_a = 0.0254 m
	Width, b_a = 0.0254 m
	Thickness, t_a = 0.000254 m
	Dielectric const., ε_{33} = 1.5 x 10^{-8} Farad/m
	Dielectric loss factor, δ = 0.000

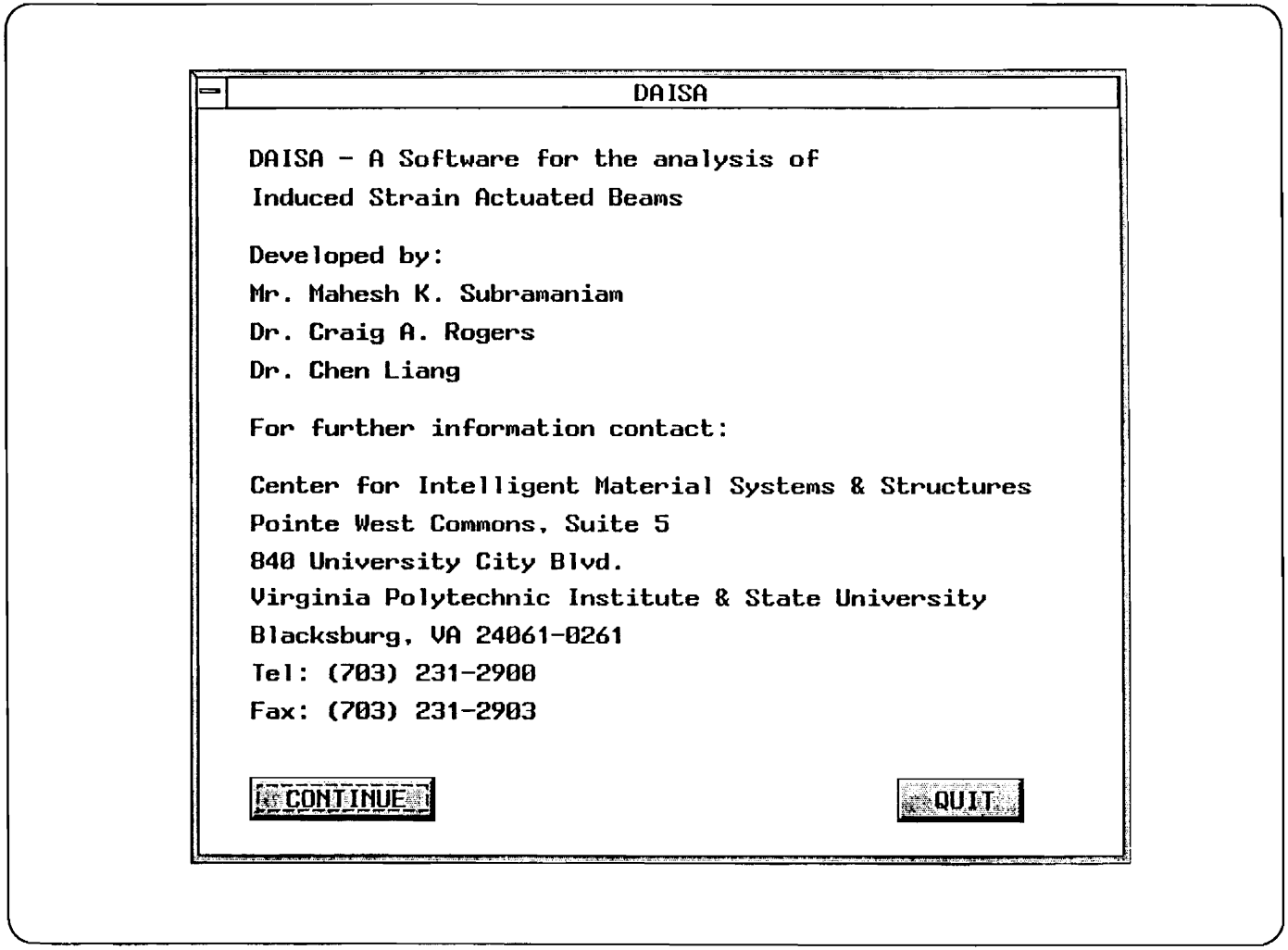

Figure 4.1 : Initial Dialog Window

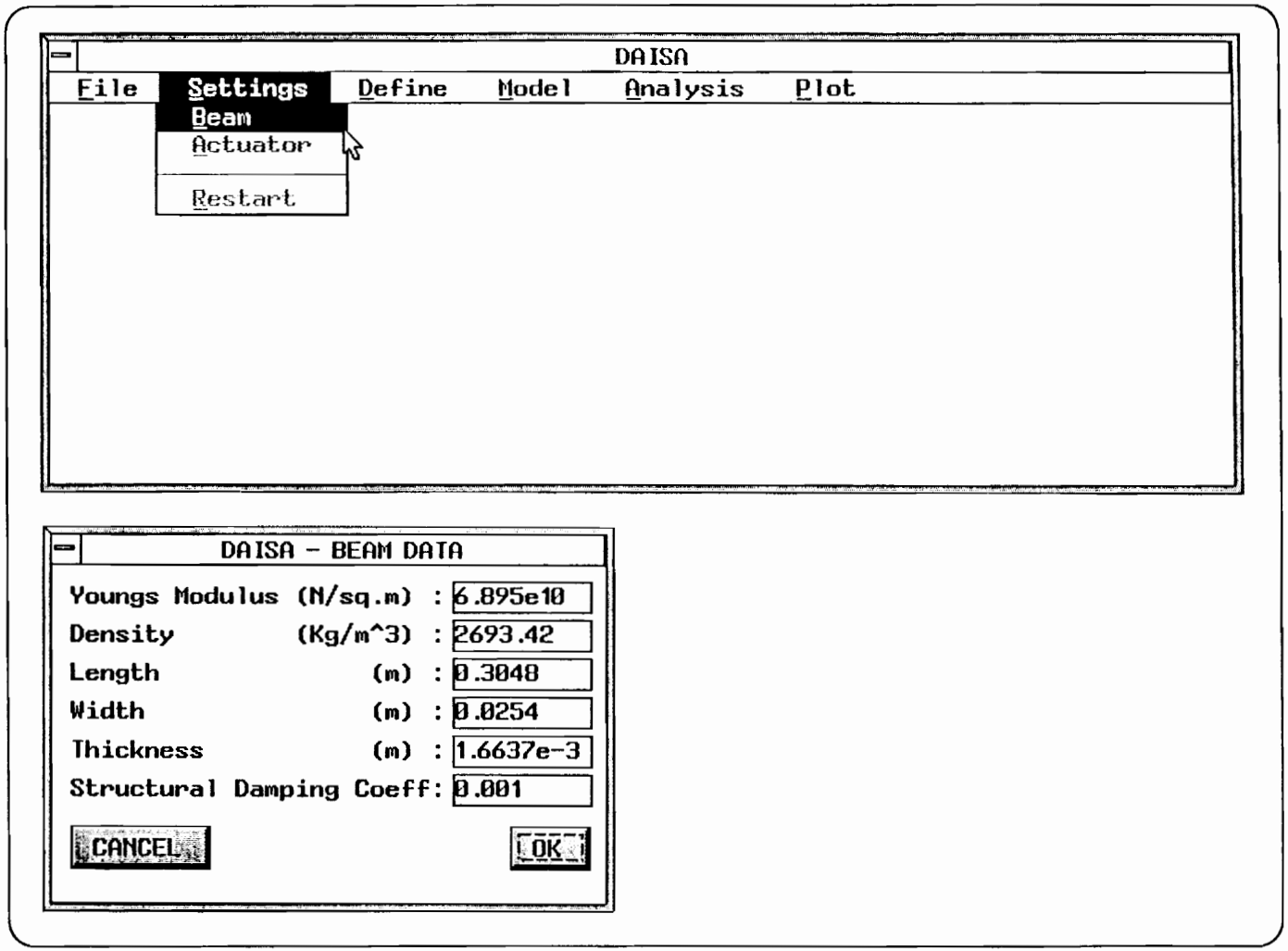

Figure 4.2 : Beam Property Settings

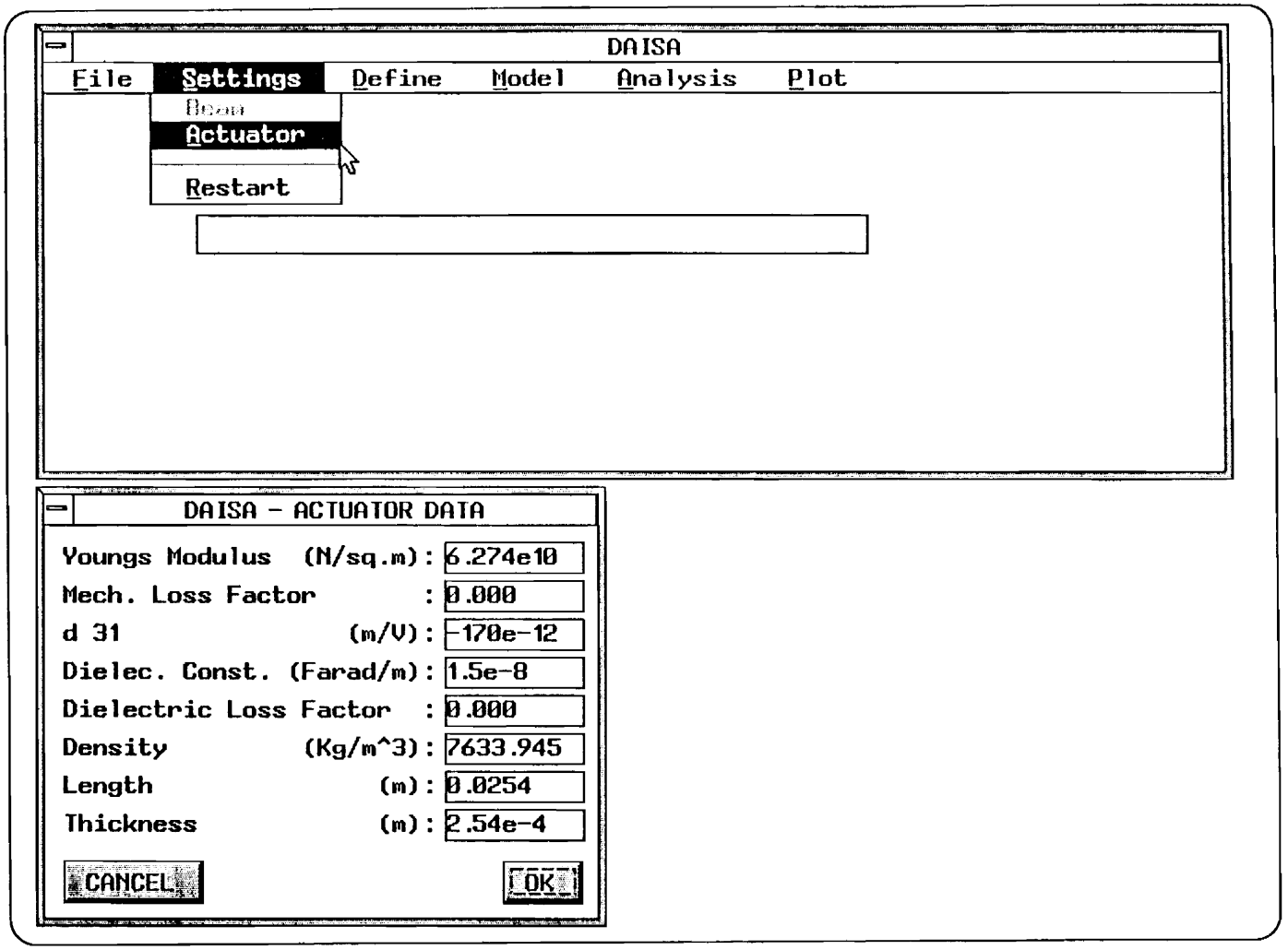

Figure 4.3 : Actuator Property Settings

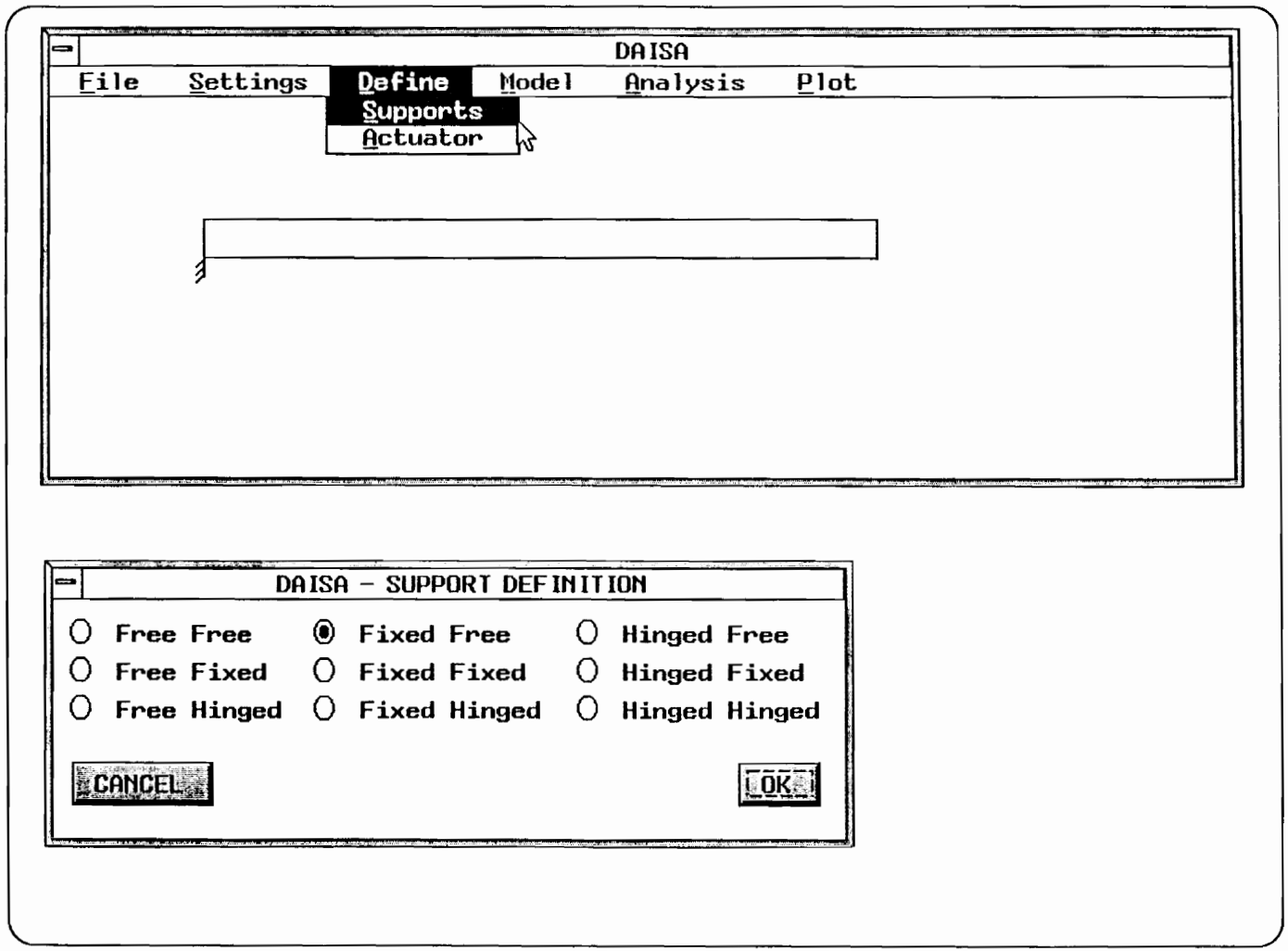

Figure 4.4 : Boundary Conditions Definition

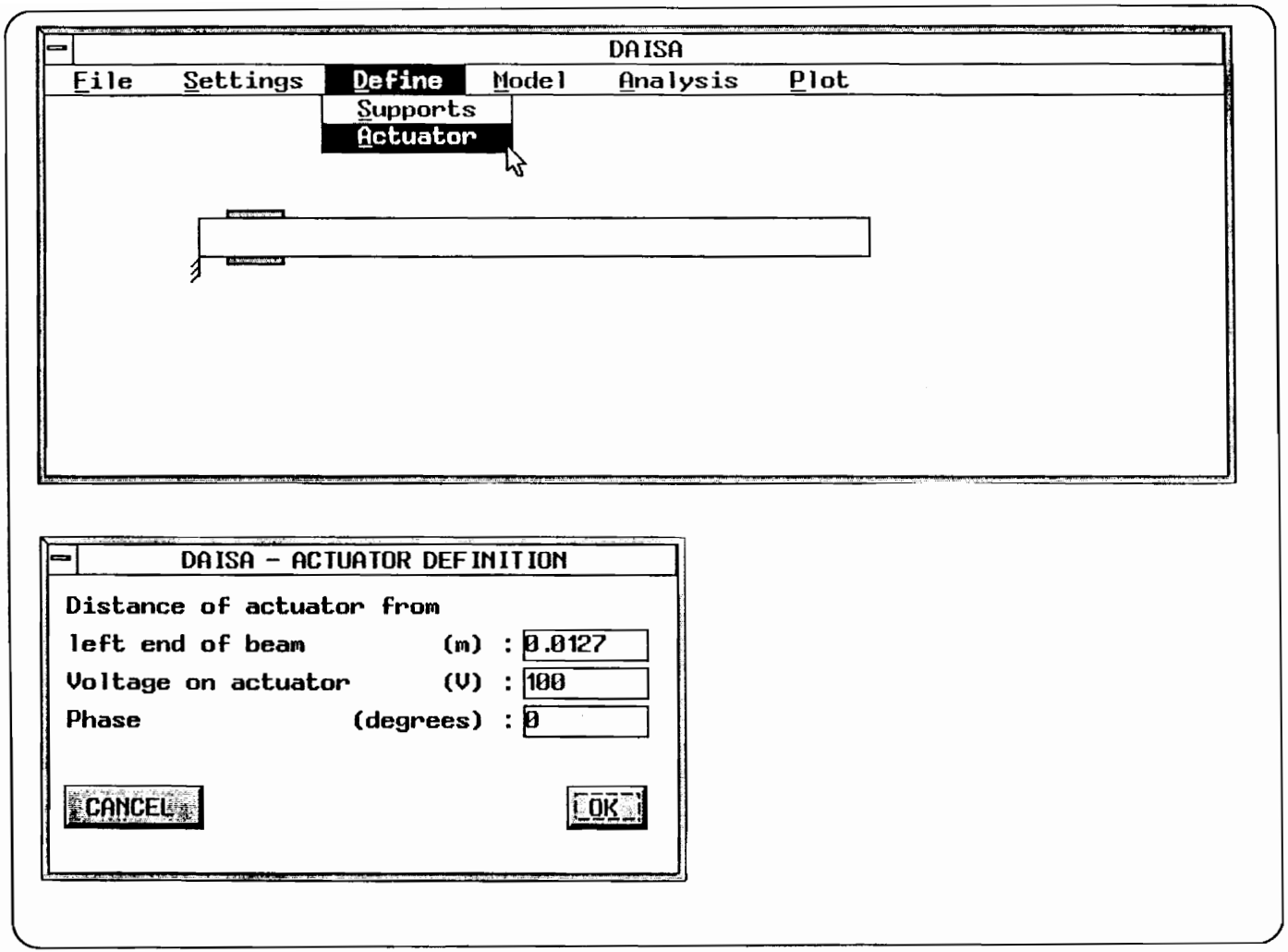

Figure 4.5 : Actuator Location, Activation Level Definition

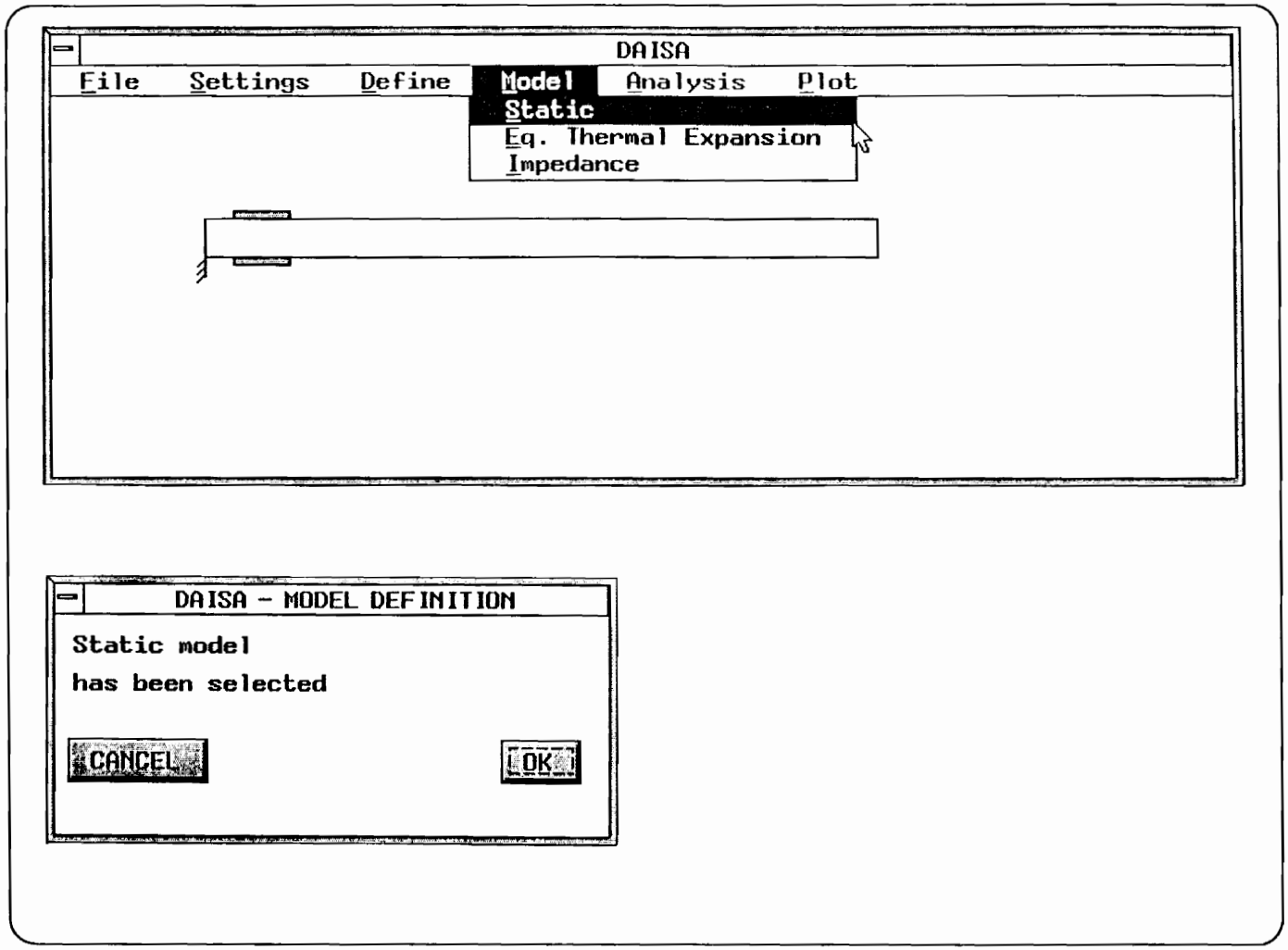

Figure 4.6 : Static Model Selection

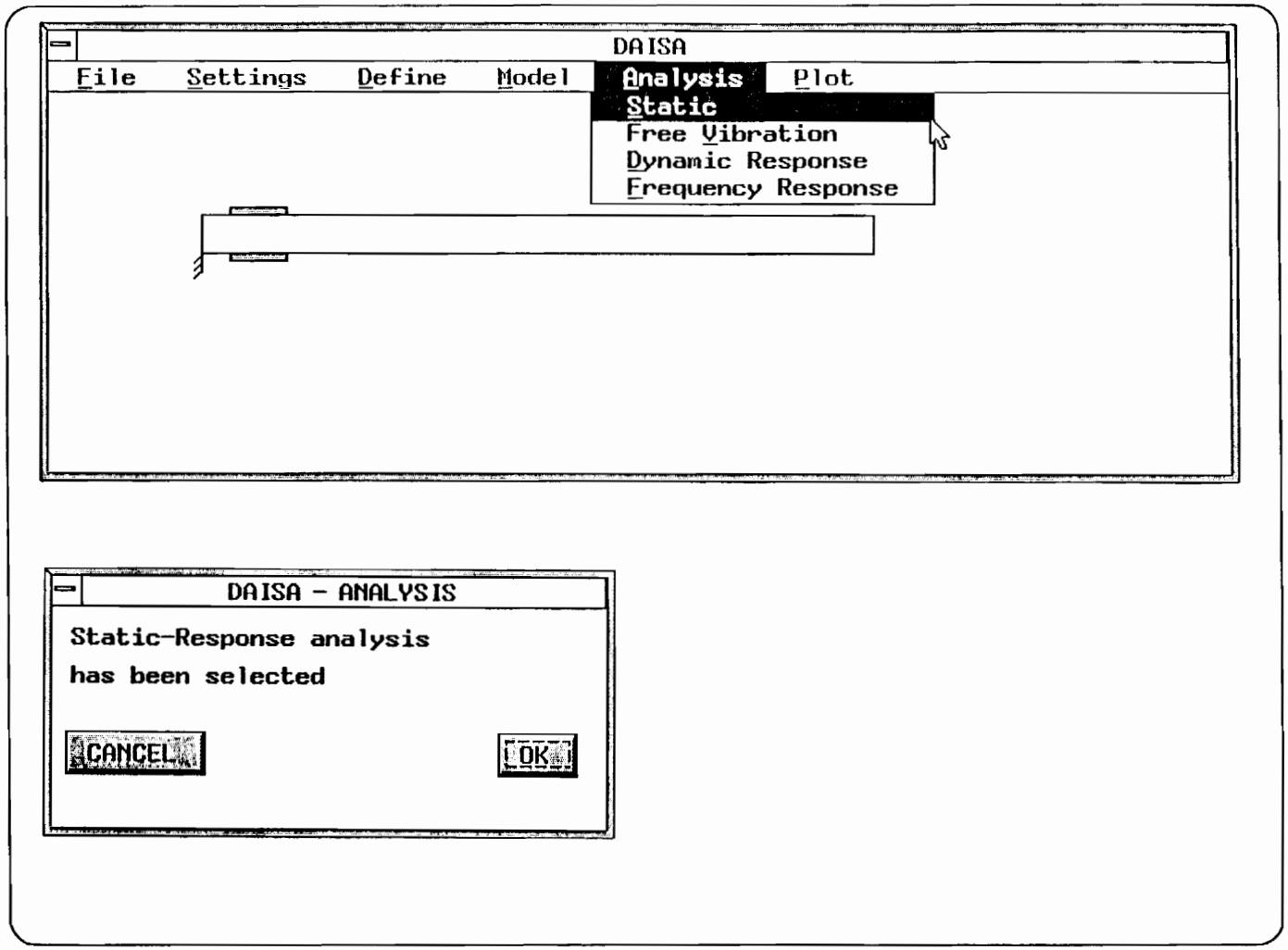

Figure 4.7 : Static-Response Analysis Selection

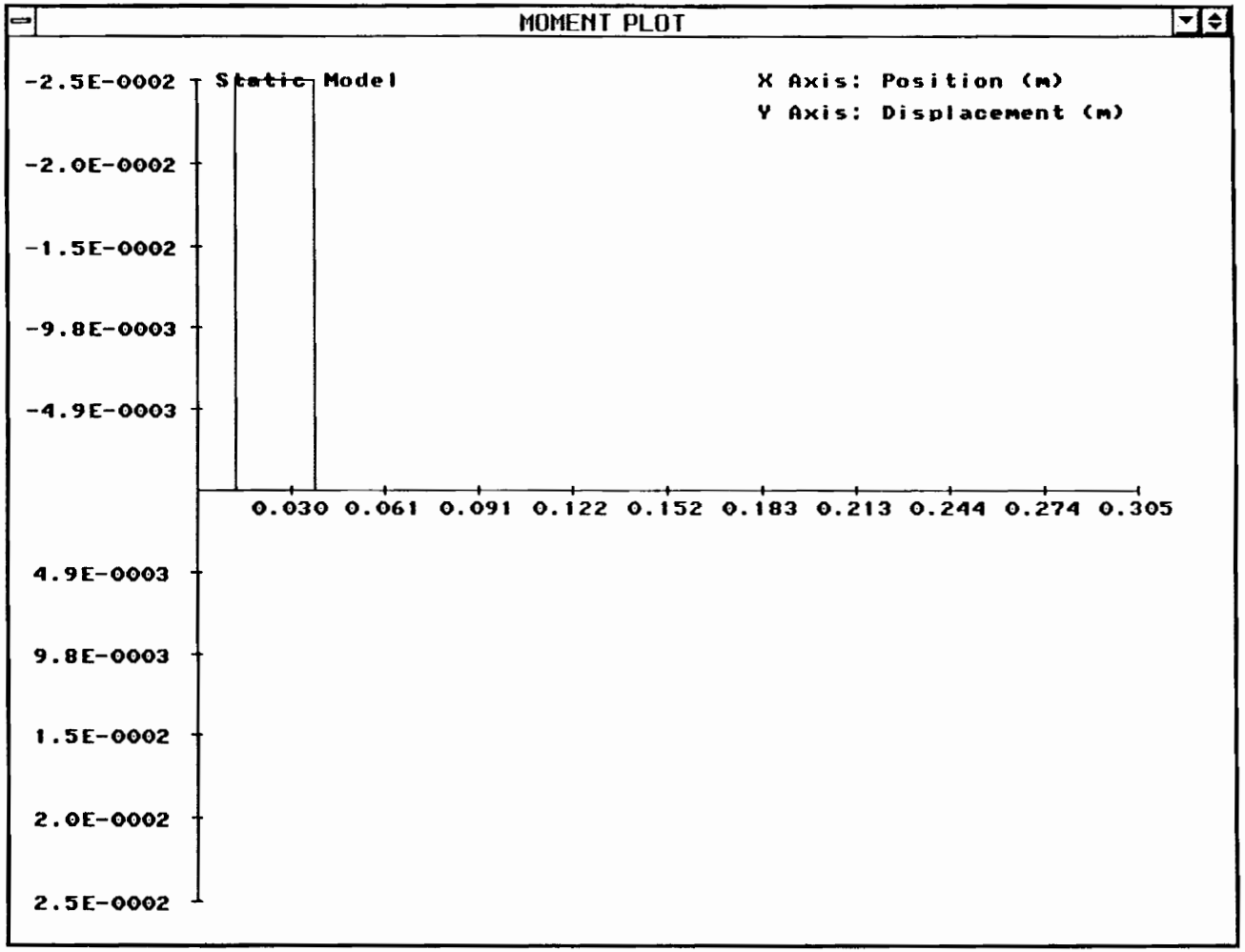

Figure 4.8 : Static Moment Plot

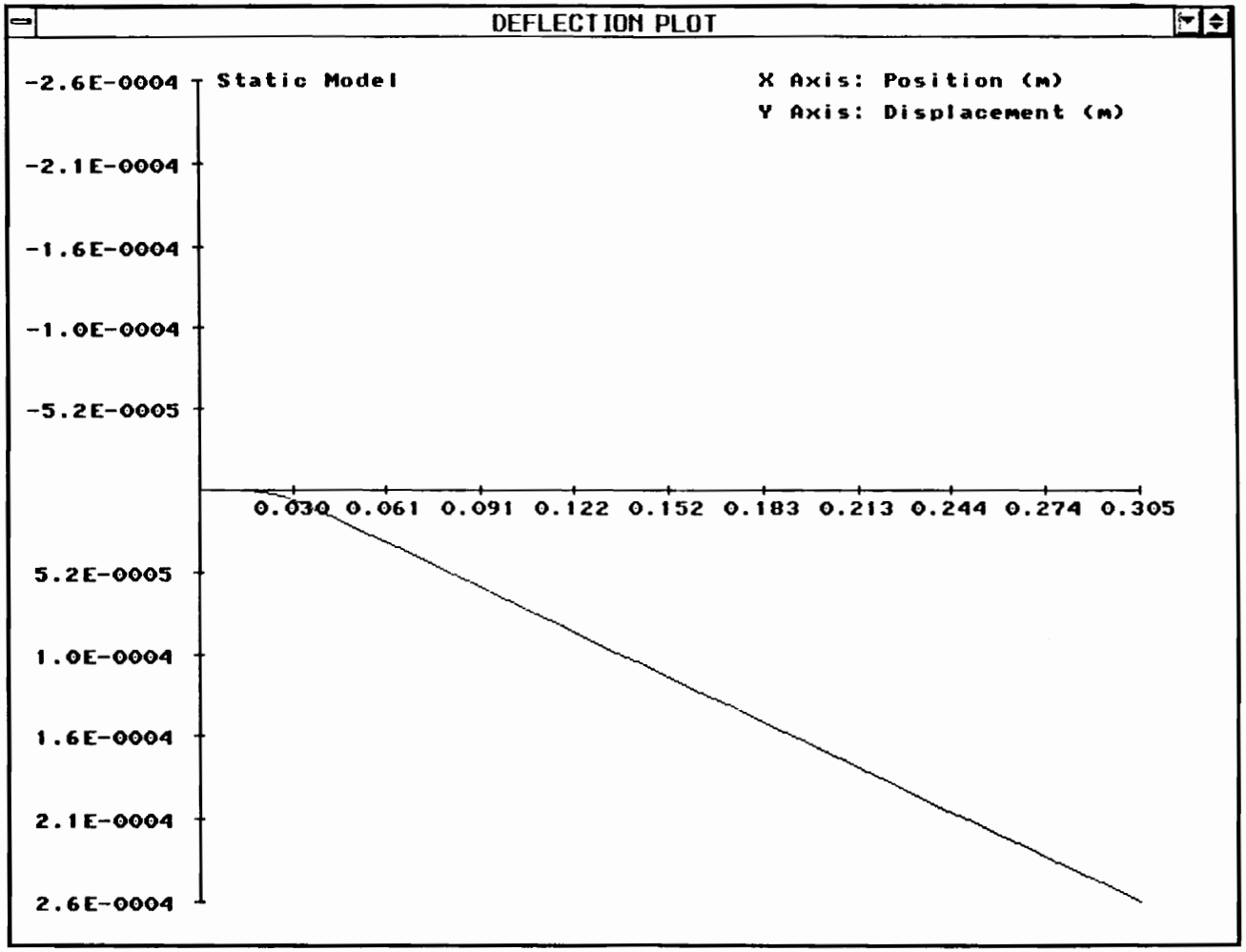

Figure 4.9 : Static Deflection Plot

Figure 4.10 shows the selection of the equivalent thermal expansion model. With this model, a free-vibration analysis is performed to obtain the natural frequencies of the material system as shown in Figure 4.11.

With the same model, a steady-state harmonic-response analysis of the material system is sought at an excitation frequency of 100 Hz as shown in Figure 4.12. The dynamic-response plot is provided in Figure 4.13.

Figure 4.14 shows the selection of the impedance model. A frequency-response analysis is sought at the center of the beam over the frequency range 0-500 Hz as shown in Figure 4.15. Associated graphical plots are provided in Figures 4.16 through 4.19.

This tutorial problem has provided a good insight into the use of DAISA. The implementation of the various models and analyses follow the discussions in the previous sections. Besides using the results of the calculation to provide graphical plots within DAISA, an output file is also written for every analysis. This output file can be imported easily to any graphing software like Matlab™ for further calculations and graphing.

Figure 4.20 provides a comparison of DAISA and BEAM VI (Mitchell, 1991) results for the frequency-response analysis discussed earlier. It can be seen that the solutions agree very well. Solutions for other models and analyses also compare well with BEAM VI results.

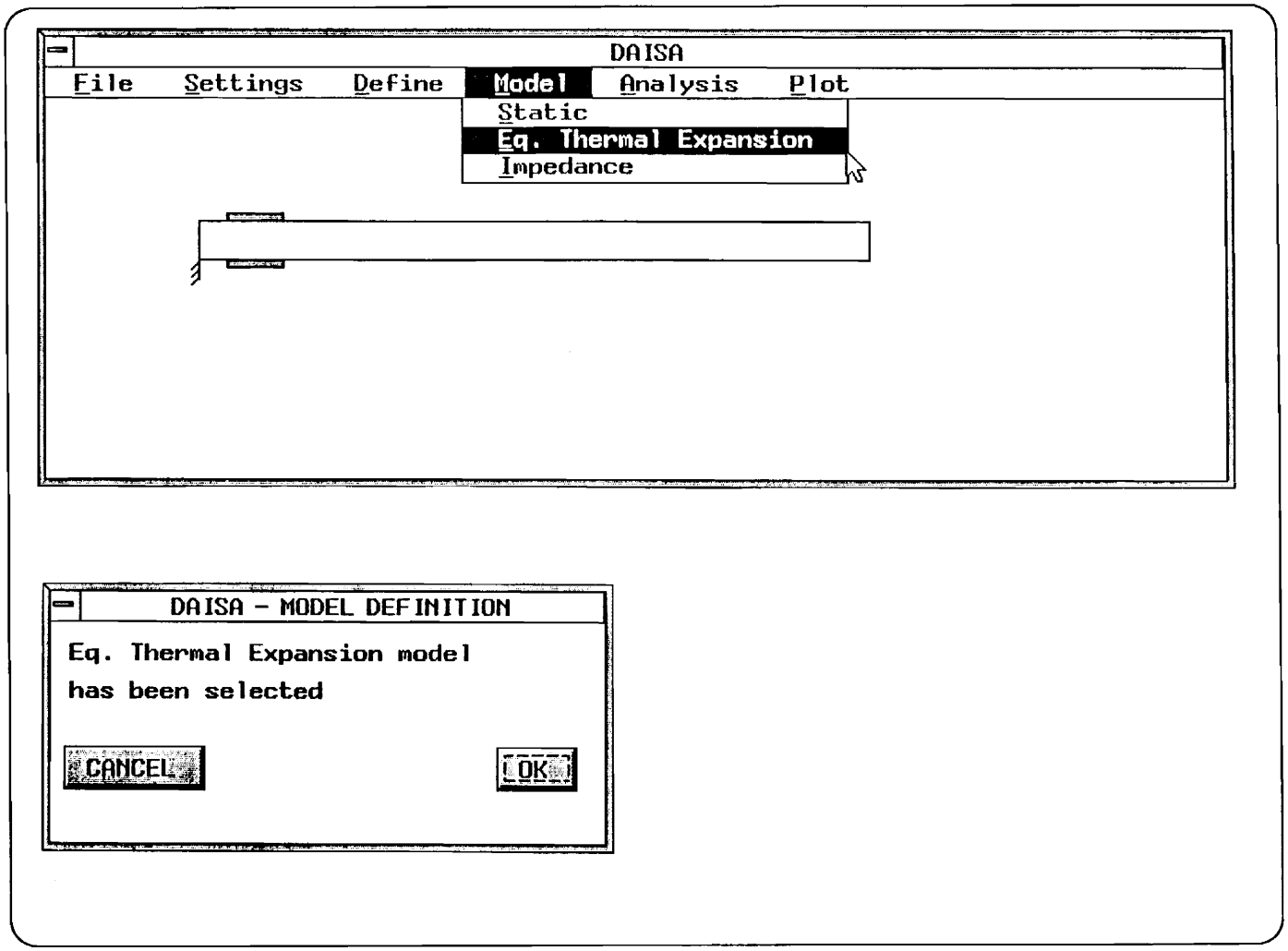

Figure 4.10 : Equivalent Thermal Expansion Model Selection

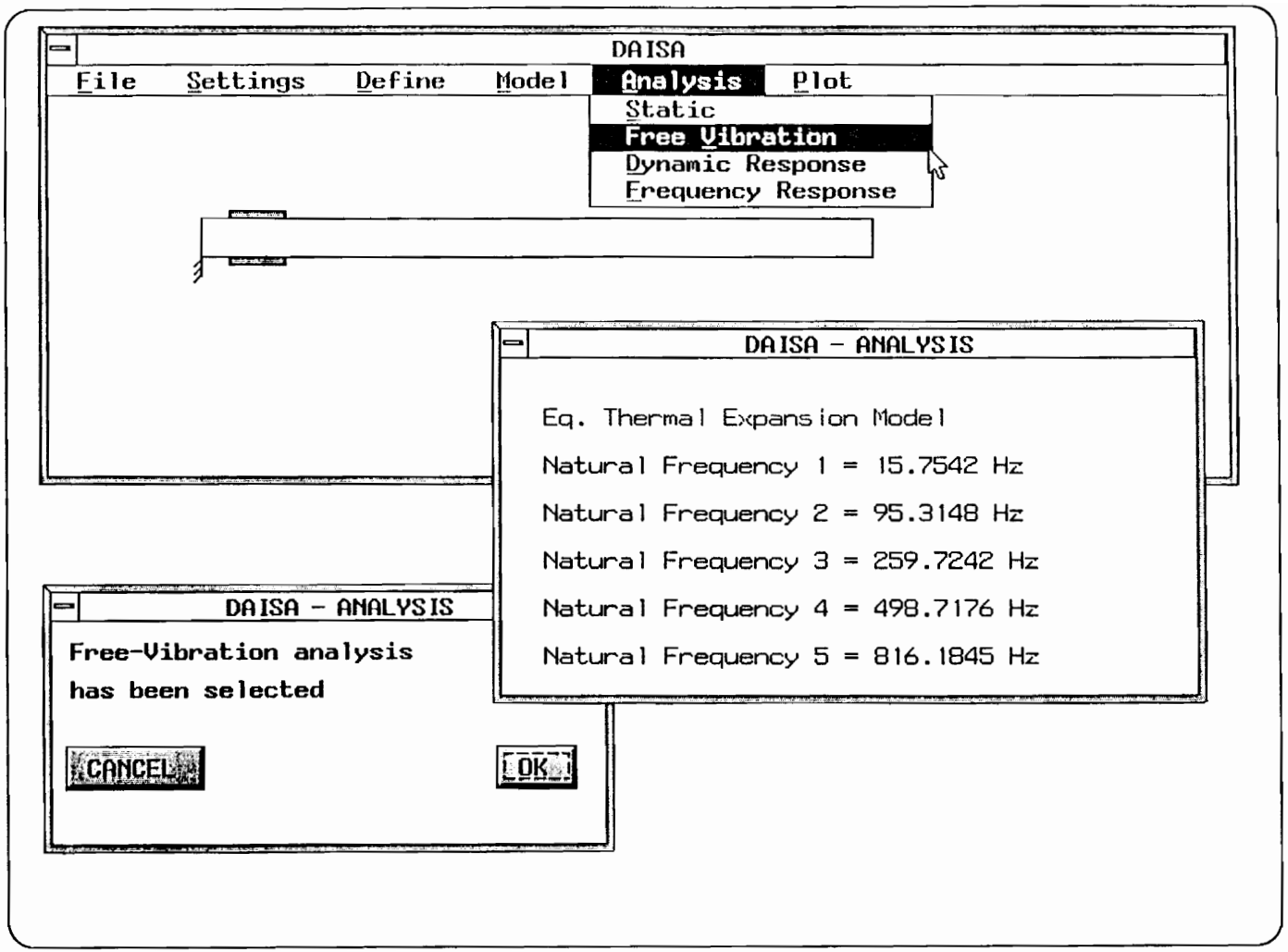

Figure 4.11 : Free-Vibration Analysis Selection

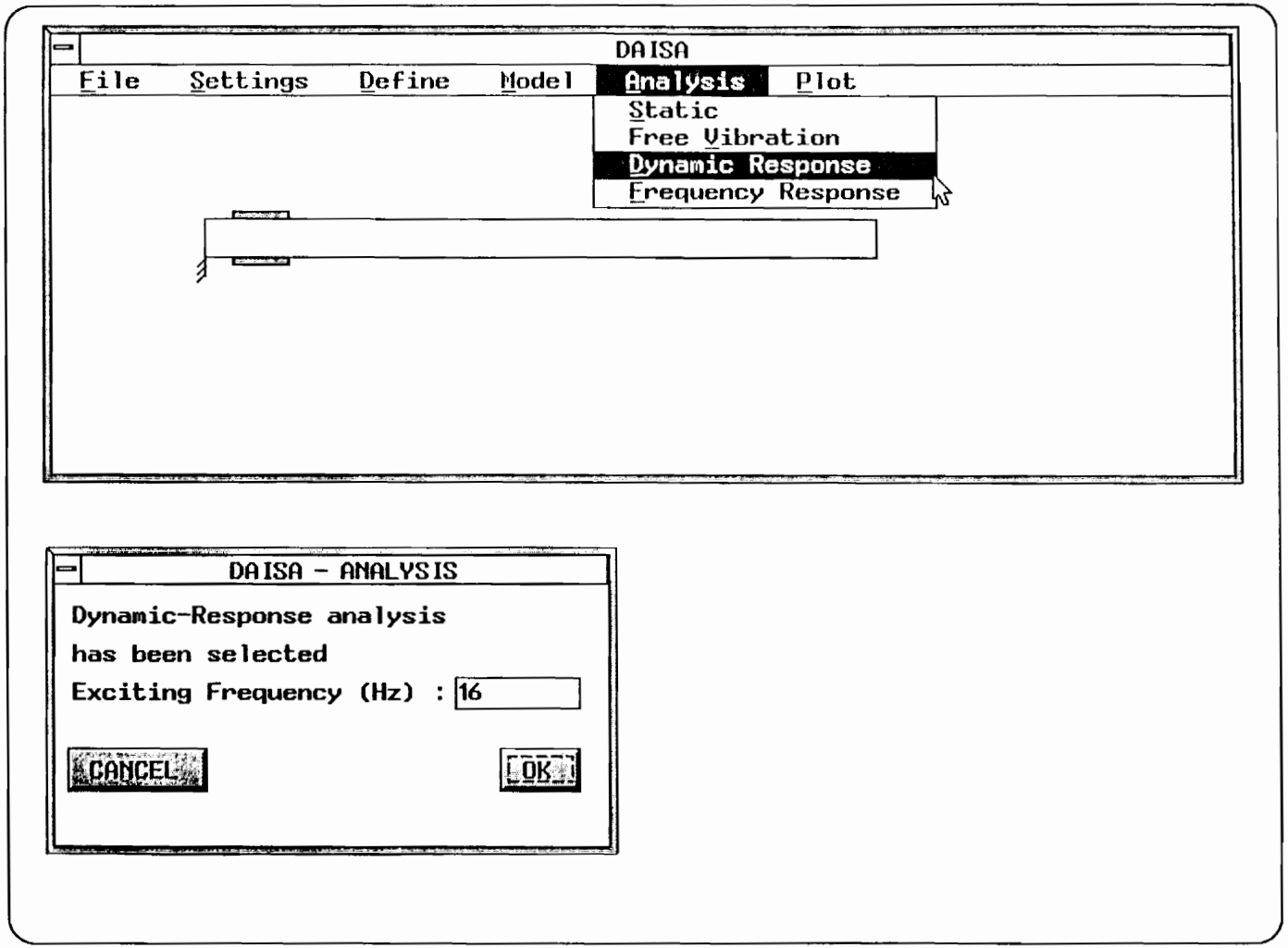

Figure 4.12 : Dynamic-Response Analysis Selection

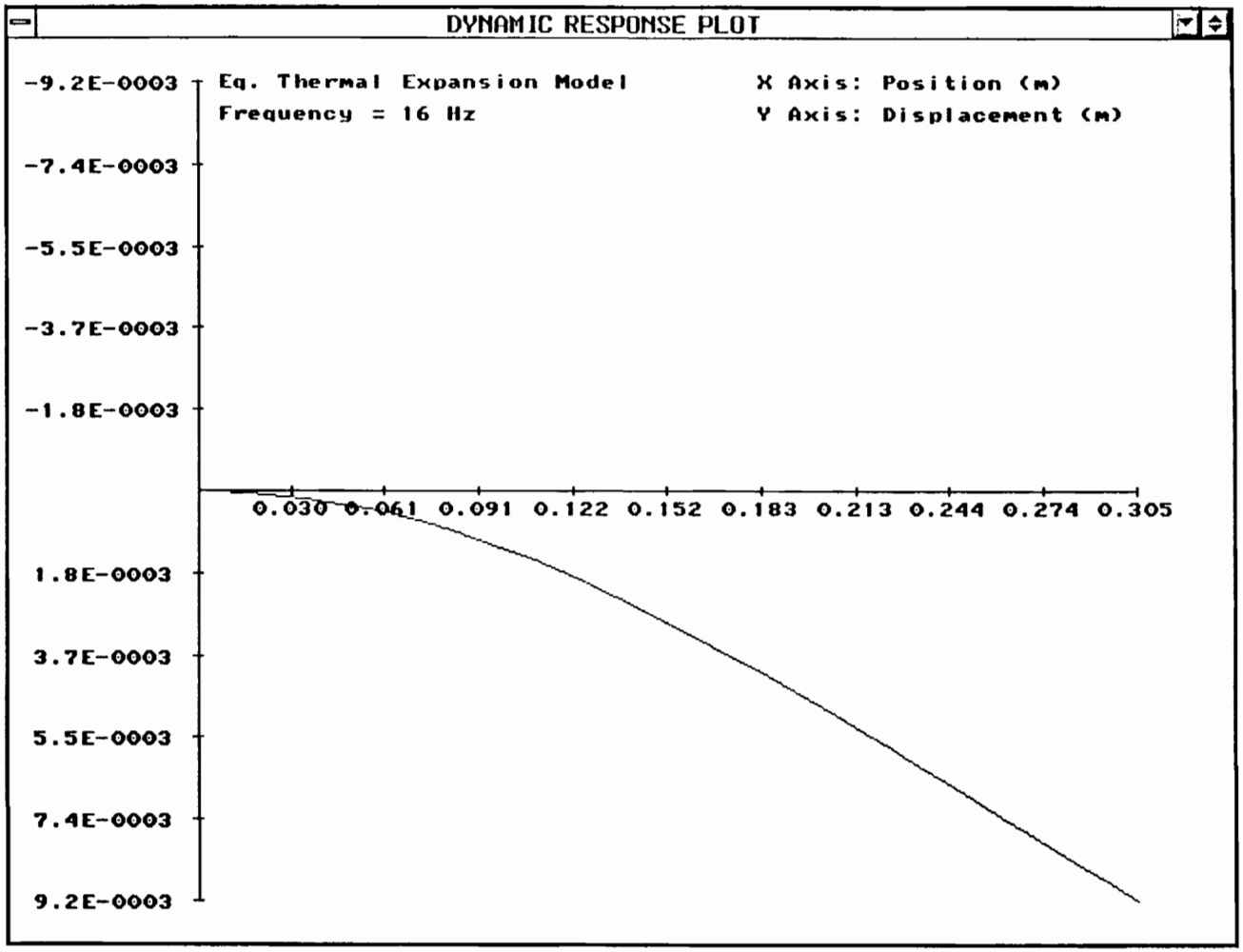

Figure 4.13 : Dynamic-Response Plot

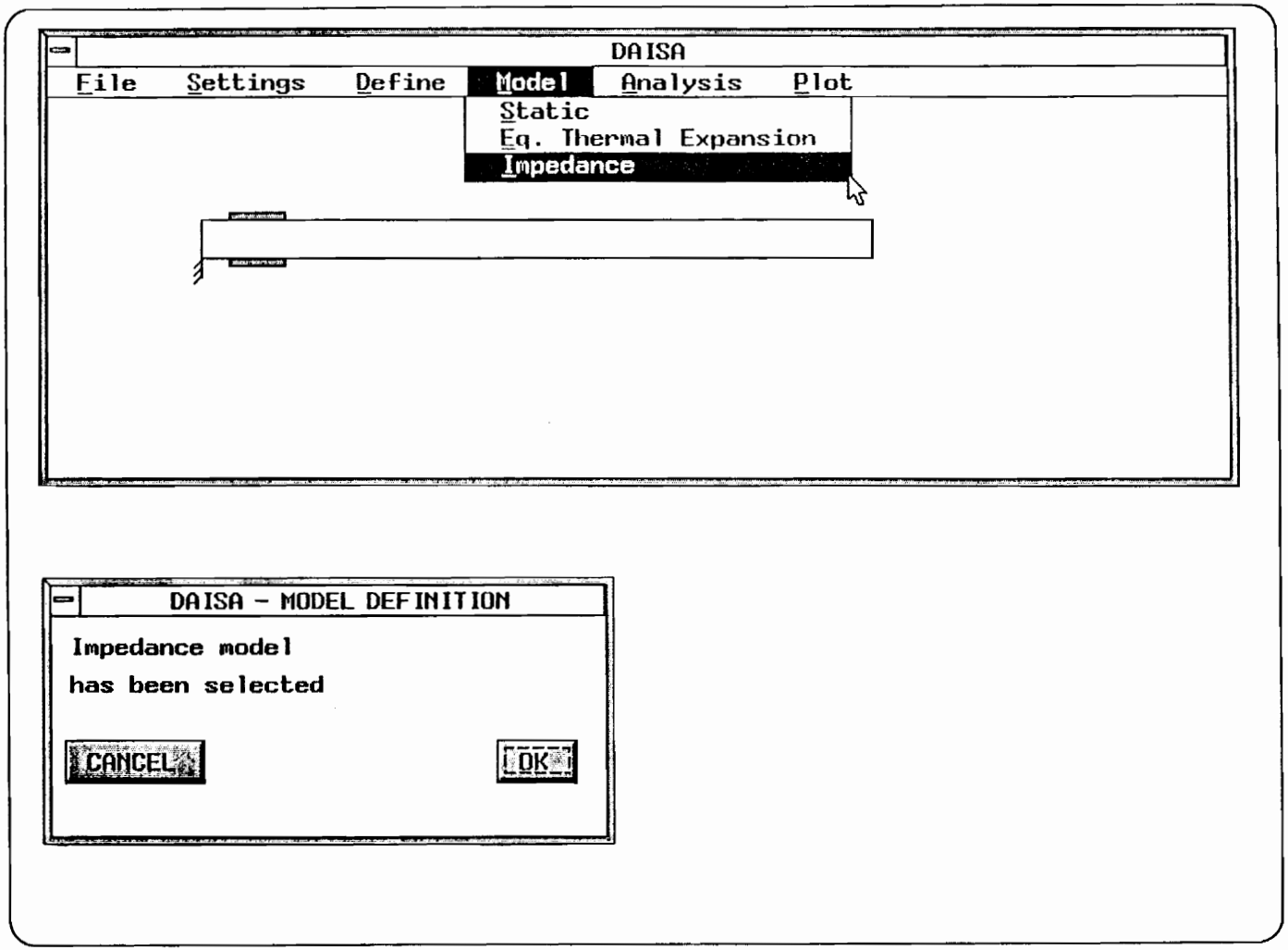

Figure 4.14 : Impedance Model Selection

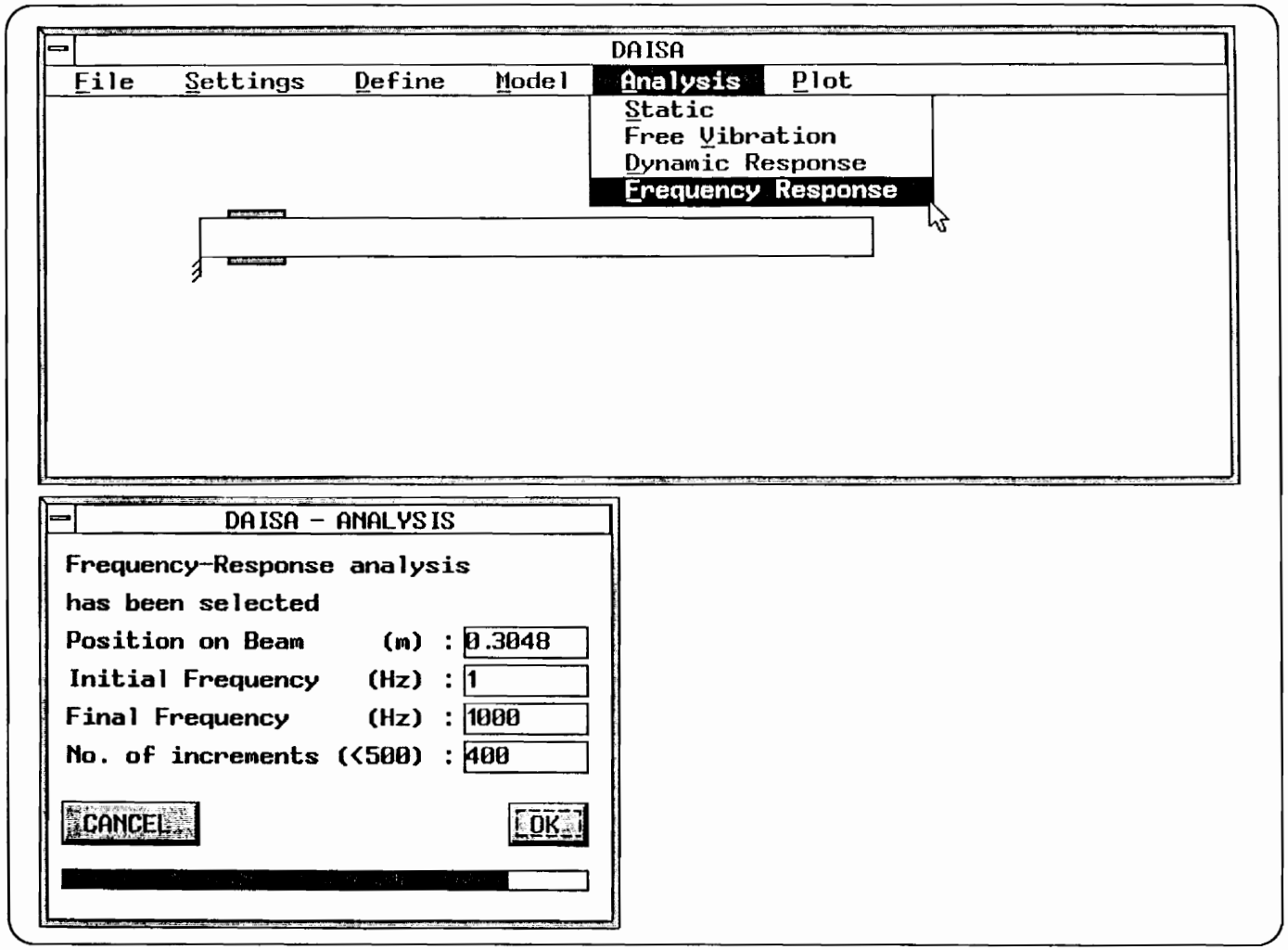

Figure 4.15 : Frequency-Response Analysis Selection

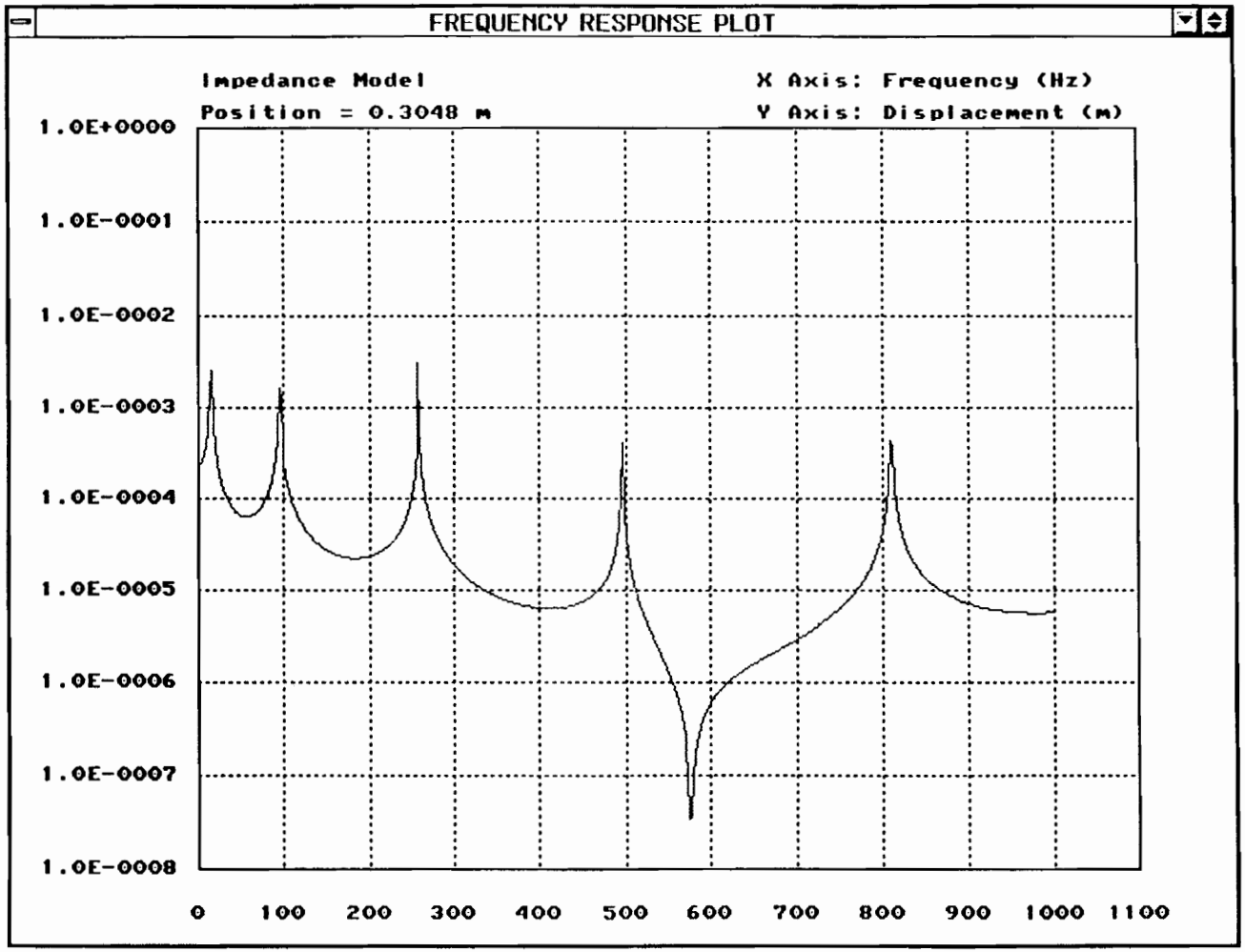

Figure 4.16 : Frequency-Response Plot

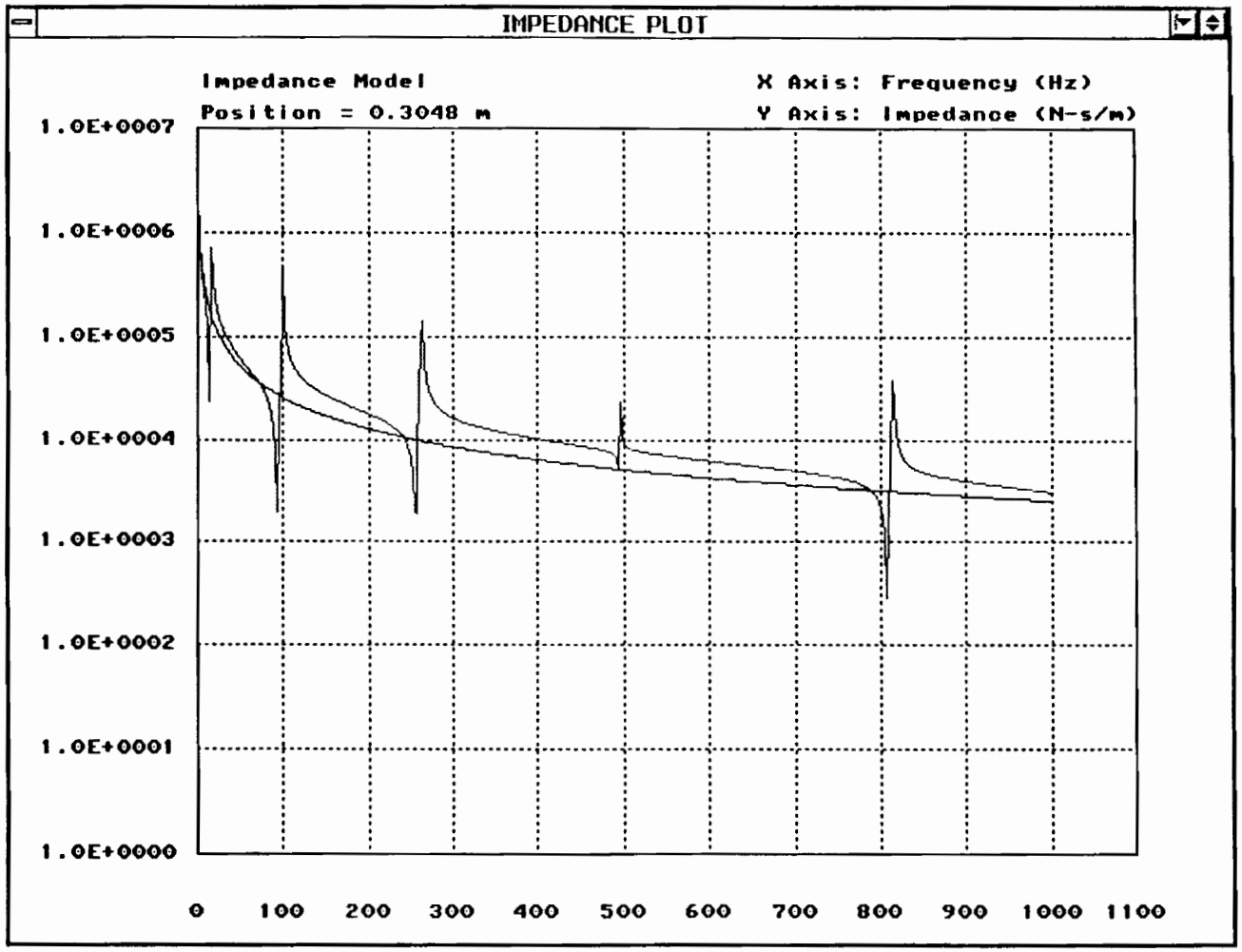

Figure 4.17 : Structural Impedance, Actuator Impedance Plot

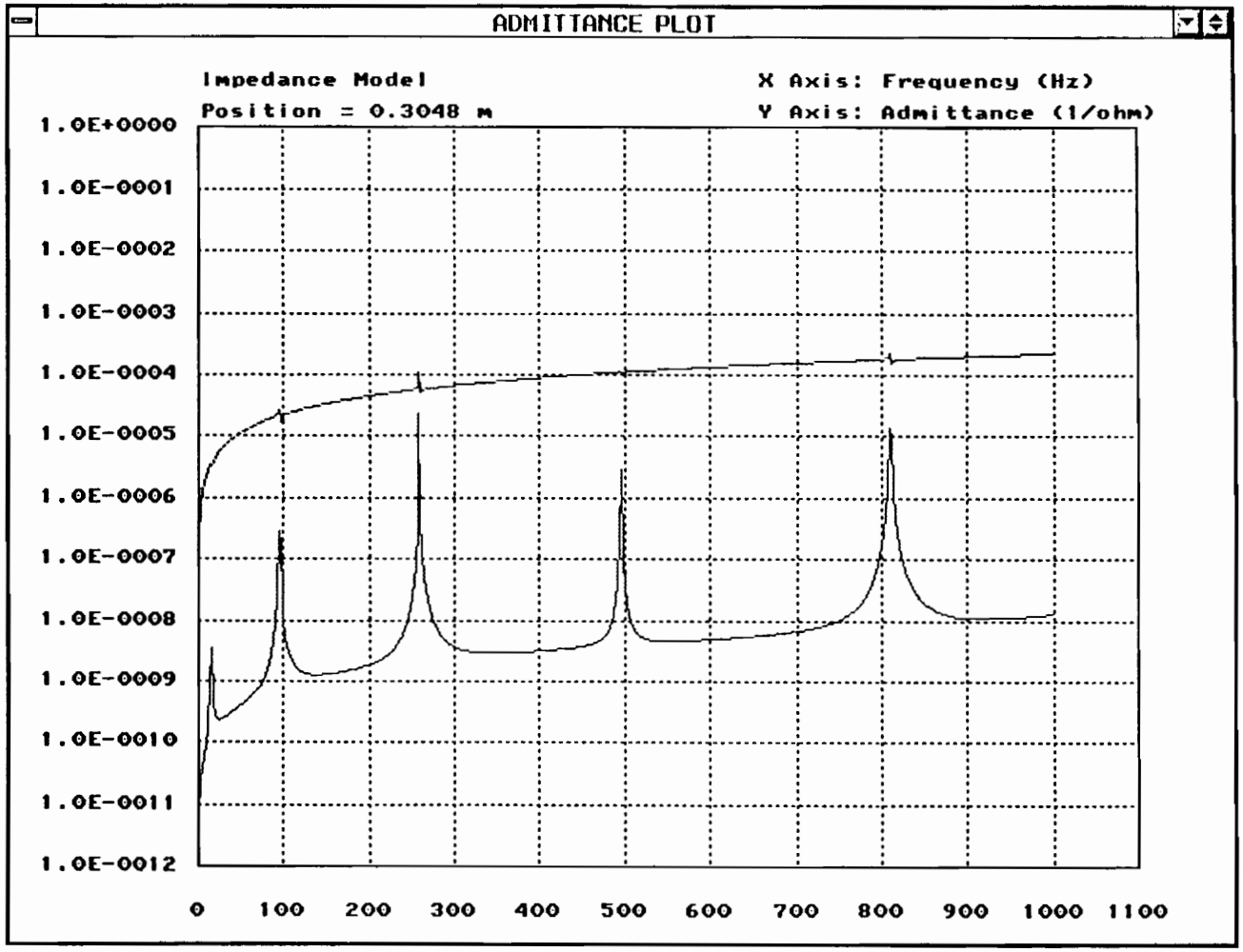

Figure 4.18 : Admittance Plot

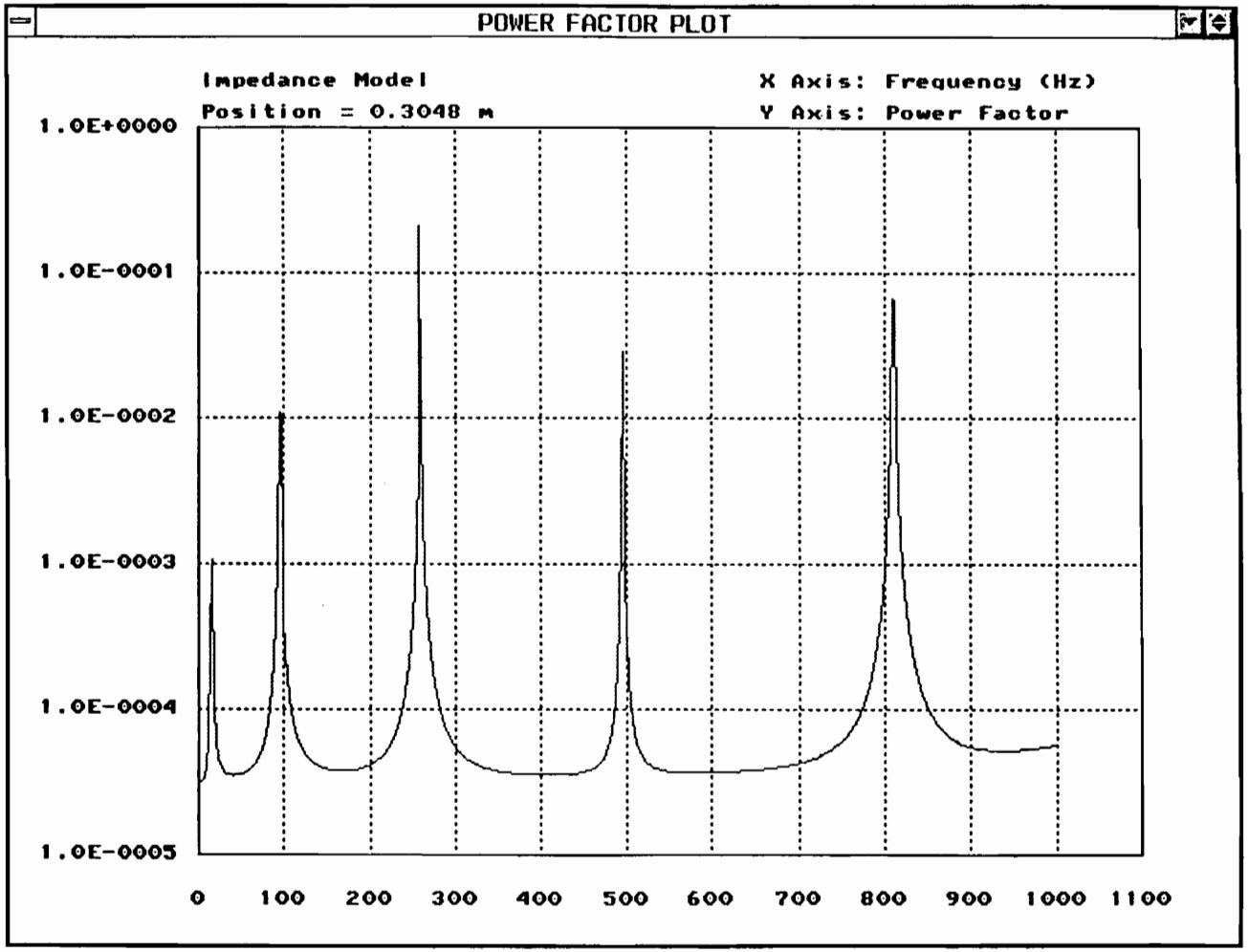

Figure 4.19 : Power Factor Plot

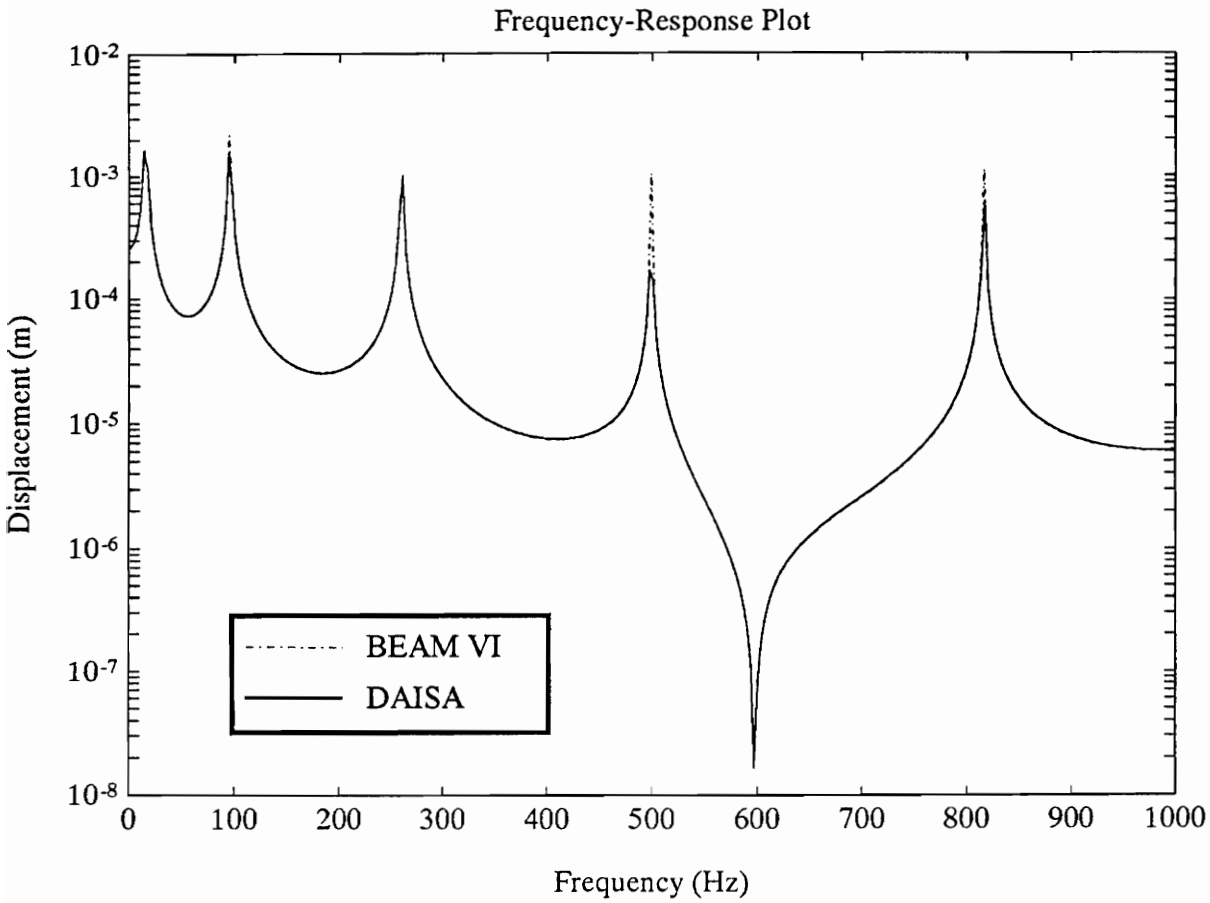

Figure 4.20 : Comparison of DAISA and BEAM VI Frequency-Response Analysis Results

Chapter 5

Conclusions and Recommendations

5.1 Conclusions

A generalized solution technique and an associated computer implementation scheme for the static and dynamic analysis of induced strain actuated beam structures have been presented in this thesis. Transfer matrices have been used for generalizing the beam problem to accommodate different boundary conditions, loading conditions, mass loading, stiffening, and structural damping effects. Analyses such as static-response, free- vibration, steady-state harmonic-response, and frequency-response have been incorporated. Static, equivalent thermal expansion, and impedance models have been incorporated to enable comparison of solutions for various analyses and appreciation of the merits and demerits of using one over another for typical configurations and applications. The computer software developed for the analysis, DAISA, has been designed with a major emphasis on a highly user-friendly interface, ease of use and interpretation of analysis results. Solutions for various actuator-structure configurations have been compared with BEAM VI (Mitchell, 1991) results for various analyses and are found to agree well. DAISA is expected to reduce the time taken to analyze induced strain actuated beam structures by a great extent and provide a means of analyzing complex beam-actuator systems with ease. DAISA can thus be perceived as a computer-aided design tool to design actuators for structural and vibration control applications and an optimization tool to determine optimal structure and actuator parameters.

5.2 Recommendations

DAISA has been tested rigorously for possible errors and accuracy, consistency of solutions. The following features can be incorporated in DAISA with ease and are considered possible extensions of this thesis work.

- Use of different actuator materials

  DAISA has been designed with the linear PZT constitutive relation. This restricts the analysis to PZT actuators only. However, other actuator materials such as shape memory alloys can also be included along with associated constitutive relations. This requires generalization of the preprocessor module accounting for the physical and material properties of the actuator material.

- Use of composite beams

  This requires the substitution of the flexural stiffness in the governing differential equation of the beam with the equivalent bending stiffness as calculated from the property matrices of the composite structure.

- Activation levels other than pure extension or pure bending

  This requires the discretization of the actual loading into equivalent force causing extension and moment pairs causing bending. The overall response of the system will correspond to a superposition of the individual solutions.

- Unsymmetric actuators

  This requires the use of the corresponding constitutive relations.

References

Bailey, T., and Hubbard, J.E., 1985, "Distributed Piezoelectric-Polymer Active Vibration of a Cantilever Beam", *Journal of Guidance, Control, and Dynamics*, Vol. 8, No. 5, pp. 605-611.

Chaudhry, Z., and Rogers, C.A., 1992, "A Mechanics Approach to Induced Strain Actuation of Structures", Proceedings, *Third International Conference on Adaptive Structures*, San Diego, CA.

Chaudhry, Z., and Rogers, C.A., 1991, "Bending and Shape Control of Beams using SMA Actuators", *Journal of Intelligent Material Systems and Structures*, Vol. 2, No. 4, pp. 581-602.

Crawley, E.F., and deLuis, J., 1987, "Use of Piezoelectric Actuators as Elements of Intelligent Structures", *AIAA Journal*, Vol. 25, No. 10.

Crawley, E.F., and Lazarus, K.B., 1989, *Induced Strain Actuation of Composite Plates*, GTL Report, MIT.

Crawley, E.F., and Lazarus, K.B., 1989, "Induced Strain Actuation of Isotropic and Anisotropic Plates", *AIAA Journal*, Vol. 29, No. 6.

Dimitriadis, E.K., and Fuller, C.R., 1989, "Piezoelectric Actuators for Noise and

Vibration Control of Thin Plates", *12th ASME Conference on Mechanical Vibration and Noise*, Montreal, Canada.

Dimitriadis, E.K., Fuller, C.R., and Rogers, C.A., 1991, "Piezoelectric Actuators for Distributed Vibration Excitation of Thin Plates", *Journal of Vibration and Acoustics*, Vol. 113, pp. 100-107.

Fanson, J.L, and Chen, J.C., 1986, "Structural Control by the use of Piezoelectric Active Members", *Proceedings of NASA/DOD Control-Structures Interaction Conference*, NASA CP-2447, Part II.

Liang, C., Sun, F.P., and Rogers, C.A., 1993a, "An Impedance Method for Dynamic Analysis of Active Material Systems", Submitted to the *ASME Journal of Vibration and Acoustics*.

Liang, C., Sun, F.P., and Rogers, C.A., 1993b, "Coupled Electro-Mechanical Analysis of Piezoelectric Ceramic Actuator-Driven Systems - Determination of the Actuator Power Consumption and System Energy Transfer", *SPIE's 1993 North American Conference on Smart Structures and Materials*, Albuquerque, 1-4 February, 1993, in press.

Li, William, X., Mitchell, L.D., and Zeng, X., 1992, "Extraction of Complex Eigenvalues of Generally Damped Mechanical Systems: A Review", *Proceedings of IMAC 10*, San Diego, CA, pp. 614-626.

Mitchell, L.D., 1992, *User's Guide - Beam VI*, AMDF Publication, Virginia Polytechnic Institute and State University.

Pestel, E.C., and Leckie, F.A., 1963, *Matrix Methods in Elasto Mechanics*, McGraw Hill Book Company, Inc, NY.

Pilkey, W.D., 1969, *Manual for the Response of Structural Members - Volume I and II*, IIT Research Institute, IL.

TEGL Windows Toolkit for Pascal, 1991, TEGL Systems Corporation, Canada.

Wang, B.T., and Rogers, C.A., 1991, "Modeling of Finite Length Spatially Distributed Induced Strain Actuators for Laminate Beams and Plates", AIAA Paper Np. 91-1258, *Proceedings of the 32nd SDM Conference,* Baltimore, MD, pp. 1511-1520.

Vita

Mahesh Kumar Subramaniam was born in Madras, India on July 9, 1970. He received his higher secondary school certificate from Vanavani in Madras in 1987. He joined the College of Engineering at Anna University in the fall of 1987 and graduated with a B.S. degree in Mechanical Engineering in 1991. He came to Virginia Tech in the fall of 1991 and started working in the area of intelligent material systems. He graduated with a M.S. degree in Mechanical Engineering in May 1993. He is beginning his career with the Automotive Systems Group of Johnson Controls, Inc. in Plymouth, Michigan.